



Peer review status:

This is a non-peer-reviewed preprint submitted to EarthArXiv.

1 **Remote sensing and deep learning for standing dead-tree detection**
2 **and mapping: A review of advances, challenges, and future**
3 **directions**

4
5 Anwarul Islam Chowdhury^{a,b*}, Mirela Beloiu^c, Teja Kattenborn^d, Clemens Mosig^e, Mete Ahishali^b, Mikko
6 Vastaranta^a, Eetu Puttonen^f, Eija Honkavaara^f, Langning Huo^g, Md. Jamal Uddin^h, Verena C. Griess^c, Anton
7 Kuzmin^{a,i}, Yan Cheng^j, Samuli Junntila^{a,b,f}

8
9 ^a School of Forest Sciences, University of Eastern Finland, 80101 Joensuu, Finland

10 ^b Department of Forest Sciences, University of Helsinki, 00014 Helsinki, Finland

11 ^c Department of Environmental Systems Science, Institute of Terrestrial Ecosystems, ETH Zurich, 8092 Zurich,
12 Switzerland

13 ^d Sensor Based Geoinformatics, Faculty of Environment and Natural Resources, University of Freiburg,
14 Freiburg, Germany

15 ^e Institute for Earth System Science and Remote Sensing, Leipzig University, Leipzig, Germany

16 ^f Department of Remote Sensing and Photogrammetry, Finnish Geospatial Research Institute, National Land
17 Survey of Finland, 02150 Espoo, Finland

18 ^g Department of Forest Resource Management, Swedish University of Agricultural Sciences, S-901 83 Umeå,
19 Sweden

20 ^h Department of Forestry and Environmental Science, Rangamati Science and Technology University, 4500
21 Rangamati, Bangladesh

22 ⁱ Department of Geographical and Historical Studies, University of Eastern Finland, Joensuu, Finland

23 ^j Department of Geosciences and Natural Resource Management, University of Copenhagen, Copenhagen,
24 Denmark

25

26

27

28

29 * Corresponding author: anwarul.islam.chowdhury@uef.fi (Anwarul Islam Chowdhury)

30

31

32

33

34

35

36

37

38

39

40 **Abstract**

41 Standing dead trees are visible indicators of recent tree mortality and an important transitional component
42 linking forest disturbance to future lying deadwood, habitat availability, and carbon storage. As drought, insect
43 outbreaks, pathogens, and climate extremes intensify tree mortality worldwide, scalable methods are needed
44 to detect and map standing dead trees consistently across forest landscapes. Recent advances in high-
45 resolution remote sensing and computer-vision-based deep learning, including object detection, semantic
46 segmentation, instance segmentation, and transformer-based models, are making large-scale standing dead-
47 tree detection increasingly feasible. This review synthesizes 38 studies from 2019 to 2026 that apply deep
48 learning to optical and LiDAR data acquired from UAV-borne, airborne, satellite, and multi-sensor remote
49 sensing platforms for standing dead-tree detection and mapping. We identify five major advances: 1) object-
50 detection models have become central for identifying dead trees, especially where mortality is spatially
51 scattered and dead trees occur at low density, with transformer-based frameworks emerging as a promising
52 development; 2) U-Net derivatives and hybrid or ensemble models are widely used for segmentation in dense
53 canopies; 3) multi-sensor fusion can improve detection robustness, particularly where spectral and structural
54 cues are complementary; 4) transfer learning and domain adaptation are important for scaling across regions,
55 although cross-biome generalization remains limited by differences in forest structure, dead-tree appearance,
56 and sensor characteristics; and 5) model comparability is constrained by inconsistent annotations, varying
57 definitions of standing dead trees, and the lack of standardized benchmark datasets. Despite substantial
58 progress, operational deployment remains limited by canopy occlusion, class imbalance, annotation variability,
59 and uncertain transferability. By linking ecological monitoring needs with recent methodological advances, this
60 review outlines a pathway toward scalable, transferable, and benchmarked deep-learning systems for standing
61 dead-tree monitoring, supported by standardized datasets, domain-invariant and self-supervised learning, and
62 open databases such as deadtrees.earth.

63
64 **Keywords:** Tree mortality; Deadwood; Forest health; UAV; LiDAR; Multi-sensor fusion

65
66
67
68
69
70
71
72
73
74

75 **Highlights**

- 76 • Synthesizes recent deep learning advances for standing dead-tree detection and mapping.
- 77 • Object detection models support identification of scattered and low-density dead trees.
- 78 • U-Net derivatives and segmentation models are important for dense canopy conditions.
- 79 • Multi-sensor fusion and transfer learning can improve robustness and scalability.
- 80 • Standardized benchmarks are needed for operational, large-scale standing dead-tree monitoring.

81

82

83

84

85

86

87

88

89

90

91

92

93

94

95

96

97

98

99

100

101

102

103 **1 Introduction**

104 Forests cover approximately 31% of the global land surface and support a large share of global biodiversity,
105 providing habitat for about 80% of all amphibians, 75% of all birds, and 68% of all mammals (Brockerhoff et al.,
106 2017; FAO & UNEP, 2020; Mori et al., 2017). They also regulate atmospheric carbon through photosynthetic
107 sequestration, absorbing roughly 25% of anthropogenic CO₂ emissions annually (Lv et al., 2025; Pan et al.,
108 2011). However, increasing anthropogenic pressures and climate-driven disturbances including drought,
109 extreme heat, insect outbreaks, pathogens, and wildfires are intensifying tree mortality across tropical,
110 temperate, and boreal forests (Beloïu et al., 2026; Gazol et al., 2025; Hartmann et al., 2022; Seidl et al., 2017).
111 Regional patterns highlight the scale of these changes: drought-related mortality has increased across 43% of
112 Canada's boreal forests since 2002 (Junttila et al., 2024; Liu et al., 2023), while recurrent drought and compound
113 disturbances have driven mortality in tropical forests (Boulton et al., 2022; Losso et al., 2022; Walden et al.,
114 2023; Yang et al., 2018). In Europe, bark beetle outbreaks have become a dominant mortality driver, with timber
115 losses increasing from 2.9 million m³ annually during 1950–2000 to tens of millions of cubic meters during
116 recent outbreaks across Central and Northern Europe (Hartmann et al., 2025; Hlásny et al., 2021; Schelhaas et
117 al., 2003). These mortality processes generate substantial quantities of deadwood, including standing dead
118 trees, a key structural component of forest ecosystems that strongly influences biodiversity, nutrient cycling,
119 and carbon storage (Aakala et al., 2024; Harmon et al., 2020; Oberle et al., 2018).

120 Deadwood, including standing dead trees and fallen coarse woody debris, plays a central role in forest
121 ecosystem functioning (Aakala et al., 2024; Oberle et al., 2018). Deadwood increases structural complexity and
122 provides nesting, shelter, and foraging habitats for birds, bats, small mammals, fungi, and invertebrates (Jutras-
123 Perreault et al., 2023; Löfroth et al., 2023). Many associated organisms are saproxylic species dependent on
124 decaying wood and essential for decomposition and nutrient recycling processes (Rondeux and Sanchez, 2010;
125 Shannon et al., 2022). Coarse woody debris also functions as a long-term carbon reservoir, decomposing over
126 decades to centuries and contributing significantly to forest carbon storage and energy flow (Fraver et al., 2013;
127 Harmon et al., 2020; Luo et al., 2025; Zhou et al., 2007). As decomposition progresses, gradients in moisture,
128 temperature, and nutrient availability create diverse microhabitats colonized by specialized microbial and
129 fungal communities that redistribute nutrients and enrich surrounding soils (Brabcová et al., 2022; Zhang et al.,
130 2025b; Zheng et al., 2025). These processes influence regeneration, soil development, and successional
131 dynamics (Piaszczyk et al., 2019; Wijas et al., 2024), while the quantity and spatial distribution of deadwood
132 are widely recognized as key indicators of biodiversity and ecosystem integrity (Mansuy et al., 2024;
133 Merganičová et al., 2012). In this review, we focus specifically on standing dead trees, defined as upright dead
134 trees that remain visible or potentially detectable from above-canopy remote sensing data, rather than on
135 fallen deadwood or concealed deadwood components below the canopy. This focus is important because
136 standing dead trees represent a detectable transitional stage between tree mortality and the later recruitment
137 of fallen coarse woody debris, and their monitoring may help anticipate future inputs to lying deadwood and
138 broader deadwood pools that are currently difficult to observe directly from above-canopy Earth observation
139 data.

140 Despite their ecological importance, standing dead trees remain difficult to monitor consistently across large
141 spatial scales. Field inventories provide accurate measurements of standing dead trees and other deadwood
142 components but are labor-intensive, costly, and spatially limited, particularly in remote or hazardous terrain (Ni

143 et al., 2025; Zhou et al., 2024). A central challenge is that tree mortality is often gradual rather than
144 instantaneous. Trees may pass through intermediate decline stages characterized by crown thinning,
145 discoloration, partial dieback, and structural degradation before they become clearly identifiable as dead. As a
146 result, remote sensing observations may capture a continuum of canopy conditions rather than a simple
147 alive/dead distinction. This progression is illustrated in Fig. 1, which shows how mortality signatures vary across
148 decay stages and between coniferous and broadleaf species, from early spectral changes such as crown
149 discoloration to later structural changes such as crown loss and snag formation. In advanced decay stages,
150 standing dead trees may be reduced to trunk snags with little or no visible crown, making them difficult to
151 detect in medium-resolution imagery and challenging even in some high-resolution datasets.

152
153 Remote sensing therefore provides an important complementary approach for mapping forest disturbance and
154 mortality patterns over broad spatial extents, although direct detection of individual standing dead trees
155 remains constrained by sensor resolution, canopy structure, tree condition, and decay stage. Long-term optical
156 satellite missions such as MODIS, Landsat, and Sentinel-2 provide observations of forest condition and
157 disturbance dynamics through stand- or canopy-level indicators such as canopy greenness, spectral change,
158 and vegetation indices (Antoniadis et al., 2025; Campbell et al., 2020; Hall et al., 2016). However, their spatial
159 resolutions generally limit their ability to identify individual standing dead trees, meaning that mortality is often
160 inferred indirectly from aggregated canopy signals (Eliades et al., 2024). While effective for identifying large-
161 scale disturbance events, these aggregated indicators can mask fine-scale spatial heterogeneity and limit
162 ecological interpretation of mortality processes at the individual-tree scale.

163 Recent advances in high-resolution remote sensing and deep learning have substantially improved the potential
164 for detecting standing dead trees at finer spatial scales (Fig. 2). UAV and airborne imagery can provide
165 centimeter- to decimeter-scale observations of crown condition, while LiDAR adds three-dimensional structural
166 information related to canopy height, crown geometry, and gap formation (Manfreda et al., 2018; Krzystek et
167 al., 2020; Briechle et al., 2021; Polvivaara et al., 2024). Very-high-resolution satellite imagery and dense satellite
168 time series further support broader-scale monitoring, although usually at coarser spatial detail than UAV or
169 airborne data (Liu et al., 2021; Dixon et al., 2023; Schiefer et al., 2023; Shields et al., 2025). At the same time,
170 deep learning approaches, including CNN-based classification, U-Net-based semantic segmentation, object
171 detection, instance segmentation, and transformer-based models, have enabled increasingly automated
172 detection and mapping of individual standing dead trees, dead crowns, and canopy mortality patterns (Jiang et
173 al., 2023; Junttila et al., 2024; Lucas et al., 2024; Zhou et al., 2024; Möhring et al., 2025; Rahman et al., 2025).
174 These developments create new opportunities for scalable standing-dead-tree monitoring, but also raise
175 questions about sensor choice, model transferability, annotation quality, and benchmark comparability
176 (Kattenborn et al., 2021; Fassnacht et al., 2024; Yun et al., 2024; Lines et al., 2022).

177 Despite these advances, comprehensive syntheses specifically focused on standing dead-tree detection remain
178 limited. Existing reviews have addressed adjacent topics, including remote sensing of tree mortality and forest
179 health (Eliades et al., 2024; Junttila, 2025; Ni et al., 2025), broader developments in forestry remote sensing
180 and vegetation-oriented deep learning (Fassnacht et al., 2024; Kattenborn et al., 2021; Yun et al., 2024),
181 individual tree-crown detection and delineation (Zhao et al., 2023), sensor-specific perspectives on laser
182 scanning and satellite platforms (Cotrozzi, 2022; Marchi et al., 2018; Shields et al., 2025), and the ecological
183 importance of deadwood (Steinebrunner et al., 2025; Wijas et al., 2024). However, these studies do not provide

184 a dedicated synthesis of standing dead-tree detection and mapping that jointly considers ecological relevance,
 185 sensor capabilities, and algorithmic developments. As a result, important questions remain regarding how
 186 different sensors and data-fusion strategies compare, how well deep learning models generalize across biomes,
 187 how differences in standing dead-tree definitions and annotation protocols affect comparability among studies,
 188 and to what extent current approaches can support large-scale operational monitoring. More broadly,
 189 operational deployment remains constrained by several factors, including canopy occlusion, annotation
 190 variability, and limited transferability (see Section 6).

191



192

193 **Fig. 1.** Visual representation of living, declining, and dead forest trees at different decay stages for coniferous
194 a) and broadleaf b) species across forest stands, individual tree structure, and aerial imagery (~50 cm). The
195 figure highlights how mortality signatures evolve from spectral changes (e.g., crown discoloration) to structural
196 features, with late-stage snags often lacking visible crowns and becoming difficult to detect, particularly in
197 medium-resolution imagery. Adapted from Zielewska-Büttner et al. (2018). Photo credits: PC1, Anwarul
198 Chowdhury; PC2, Clemens Mosig; illustrations by Anwarul Chowdhury.

199
200 In this review, we focus on scalable detection and mapping of standing dead trees using remote sensing and
201 deep learning approaches. Specifically, we aim to (1) synthesize current datasets and remote sensing
202 technologies for standing dead-tree detection, (2) review methodological frameworks and deep learning
203 approaches applied to optical, LiDAR, UAV, airborne, satellite, and multi-sensor data, (3) evaluate ecological
204 and management implications of spatially explicit standing dead-tree information, and (4) identify research
205 gaps and priorities for developing scalable standing dead-tree monitoring systems.

206 207 **2 Literature search and study selection**

208 We reviewed 38 studies published, accepted, or publicly released between 2019 and 2026 that applied deep
209 learning to remotely sensed data for standing dead-tree detection, segmentation, classification, or mapping.
210 Literature was retrieved from Scopus and Google Scholar. The literature search was conducted in December
211 2025 and updated in February 2026; therefore, the review includes studies available up to February 2026. In
212 Scopus, the search was applied to titles, abstracts, and keywords using the following search string: TITLE-ABS-
213 KEY ("dead tree*" OR "deadwood" OR "tree mortality") AND TITLE-ABS-KEY ("deep learning" OR "neural
214 network" OR "CNN") AND TITLE-ABS-KEY (detection OR segmentation OR mapping) AND TITLE-ABS-KEY ("aerial
215 image*" OR "laser scanning" OR "lidar" OR "UAV" OR multispectral OR satellite OR hyperspectral OR "remote
216 sensing"). In Google Scholar, simplified combinations of the terms "dead tree", "deadwood", "tree mortality",
217 "deep learning", "neural network", "CNN", "detection", "segmentation", "mapping", "aerial imagery", "laser
218 scanning", "LiDAR", "UAV", "multispectral", "hyperspectral", "satellite", and "remote sensing" were used
219 because Google Scholar does not support the same structured Boolean syntax as Scopus. Google Scholar results
220 were screened in order of relevance until no additional eligible studies were identified within the retrieved
221 records.

222 The database searches retrieved 139 records, including 59 from Scopus and 80 from Google Scholar. After
223 removing duplicates and clearly irrelevant records, 65 records were retained for title and abstract screening.
224 Seven records were excluded at this stage. The remaining 58 full-text records were assessed for eligibility, and
225 20 were excluded because they did not meet the inclusion criteria (Table A1). The final review included 38
226 studies. Studies were included if they applied a deep learning method, used remotely sensed data, and focused
227 on detecting, segmenting, classifying, or mapping standing dead trees, dead-tree crowns, snags, or canopy
228 mortality related to standing dead trees. Studies were excluded if they did not apply deep learning, did not use
229 remotely sensed data, focused only on fallen deadwood, addressed general forest disturbance without standing
230 dead-tree detection, or lacked sufficient methodological detail.

231 For each selected study, we extracted information on biome or forest type, spatial resolution, sensor modality,
 232 remote-sensing platform, model architecture, task type, validation approach, and reported performance
 233 metrics where available. Screening and data extraction were conducted by the lead author. Ambiguous cases,
 234 particularly studies addressing broader forest disturbance or canopy mortality, were discussed with co-authors
 235 when needed. Together, the selected studies show a rapid expansion of deep-learning-based standing-dead-
 236 tree monitoring across sensors, spatial resolutions, forest types, and modelling approaches. Because this
 237 review synthesizes studies with different sensors, annotation units, validation designs, and performance
 238 metrics, quantitative comparisons are interpreted descriptively rather than as direct benchmark-based
 239 rankings.

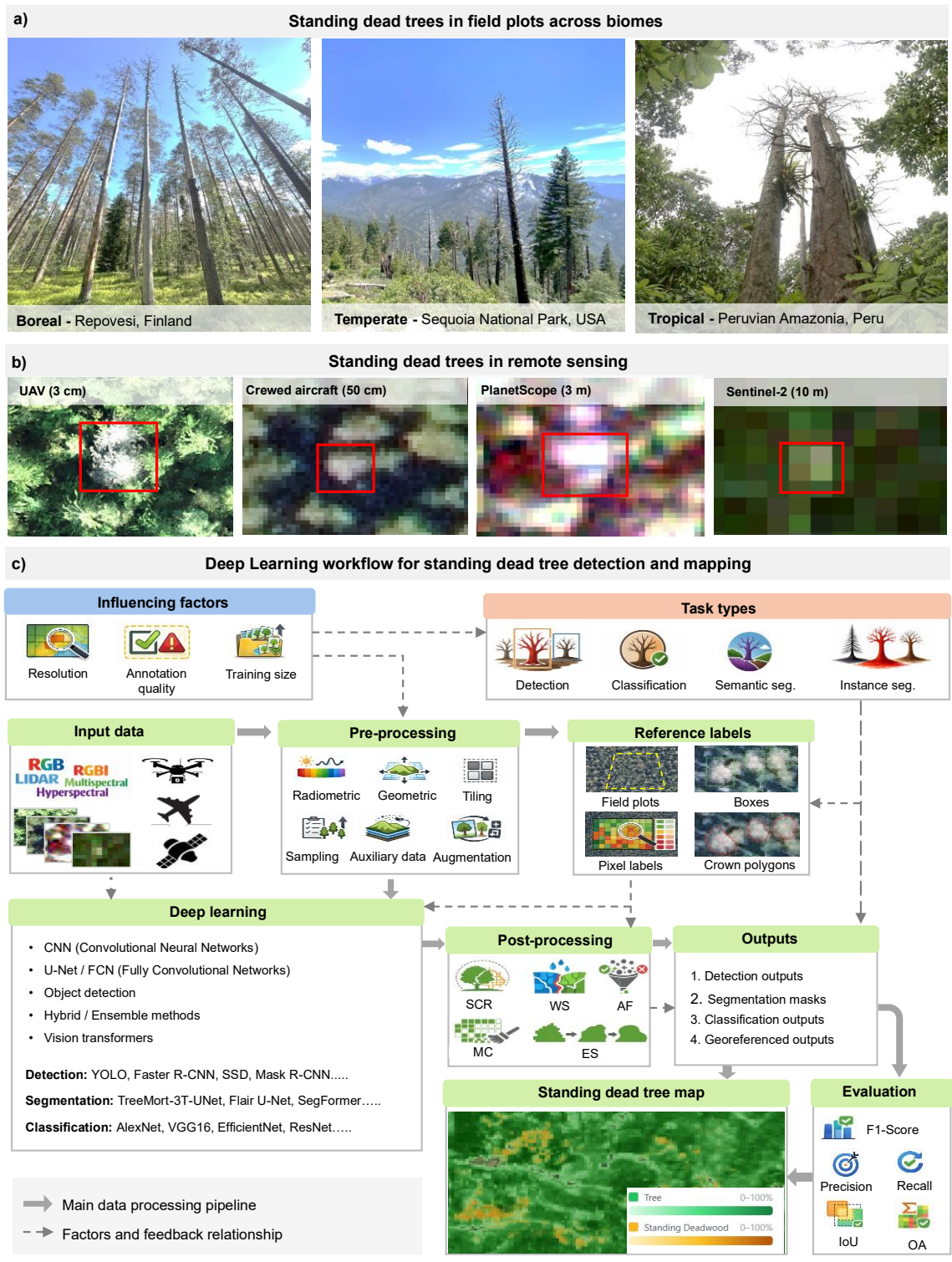
240

241 **Table 1.** Overview of studies included in the review for standing dead-tree detection and mapping. Spatial
 242 resolution is reported where available; NR indicates values not reported numerically.

No	Study	Biome/ Forest	Spatial resolution / GSD (cm)	Modality/ Bands	Models	Approach type
1	Mosig et al., 2026a	Global	1000	Multispectral	Per-pixel transformer model with HL-Gauss loss	Sub-pixel mapping
2	Ferrari et al., 2026	Temperate	10–25	RGB	SegFormer encoder + U-Net decoder	Semantic segmentation
3	Möhring et al., 2025	Global	1–28	RGB	SegFormer-B5 + U-Net decoder	Semantic segmentation
4	Mäyrä et al., 2025	Boreal	3.9–4.9	RGB + LiDAR	YOLOv8	Instance segmentation
5	Ahishali et al., 2025	Boreal / Temperate	50–60	RGBI	Flair U-Net + ADA-Net (domain adaptation)	Semantic segmentation
6	Wang et al., 2025a	Temperate	NR	RGB	DSFI-YOLO (Dual-Stream Feature Integration YOLO)	Object detection
7	Rahman et al., 2025	Boreal	25	RGBI	TreeMort-3T-UNet	Semantic segmentation
8	Yang et al., 2025	Subtropical	5–10	RGB	YOLOv5 (YOLOv5 + SE attention + BiFPN)	Object detection
9	Zhang et al., 2025a	Temperate	4	RGB	YOLOv9-ECA (YOLOv9 + Efficient Channel Attention)	Object detection
10	Leidemer et al., 2025	Temperate	1.4–2.1	RGB	YOLOv8n	Object detection
11	Gonzalez and Wallner, 2025	Temperate	20	RGBI	Attention U-Net; U-Net with ResNet34, ResNet101, EfficientNet-B7, InceptionV3 backbones	Semantic segmentation
12	Junttila et al., 2024	Boreal	50	RGBI	U-Net modification with inversed residual blocks and ASPP	Semantic segmentation

13	Wong et al., 2024	Temperate	20	LiDAR + CIR	CNN: 4 conv layers	Classification
14	Cheng et al., 2024	Temperate	25–60	RGBI	Custom EfficientUNet + deep watershed algorithm	Semantic segmentation + instance separation
15	Zhou et al., 2024	Temperate	12	RGB	Improved YOLOv7 + SimAM	Object detection
16	Matejčíková et al., 2024	Temperate	20	RGBI	CNN: 2 layers	Classification
17	Yao et al., 2024	Temperate	4	RGBI + red edge	Mask R-CNN (ResNet-50 backbone)	Instance segmentation
18	Lucas et al., 2024	Temperate	20	RGBI	Mask R-CNN (ResNet-50 + FPN backbone)	Instance segmentation
19	Khatri-Chhetri et al., 2024	Temperate	10	Multispectral + hyperspectral	CNN: 3 layers	Classification
20	Jääskeläinen, 2024	Boreal	300	RGB	U-Net	Semantic segmentation
21	Schwarz et al., 2024	Temperate	10–25	RGBI	EfficientUNet++	Semantic segmentation
22	Jin et al., 2023	Temperate	NR	RGB	Lightweight YOLOv4 (MobileNetV3 backbone)	Object detection
23	Jiang et al., 2023	Subtropical	4	RGB	Improved Faster R-CNN with Swin-Transformer backbone, FPN, and balance enhancement modules	Object detection
24	Dixon et al., 2023	Temperate	300	RGB	A custom 3D Spatio-Temporal Convolutional Neural Network	Classification
25	Schiefer et al., 2023	Temperate	6–33.9	RGB	U-Net + LSTM	Semantic segmentation + temporal modeling
26	Turkulainen et al., 2023	Boreal	3–6	RGB + multispectral + hyperspectral	2D CNN, 3D-CNN, and YOLO	Classification
27	Sani-Mohammed et al., 2022	Temperate	20	CIR	Mask R-CNN (ResNet-101 + FPN backbone)	Instance segmentation
28	Han et al., 2022	Temperate	10	RGBI	MSSCN with atrous blocks and spatial attention	Object detection
29	Wang et al., 2022	Temperate	5	RGB	LDS-YOLO	Object detection
30	Hell et al., 2022	Temperate	11–22	LiDAR + multispectral	PointCNN; 3DmFV-Net	Classification
31	Briechle et al., 2021	Temperate	10–20	LiDAR + RGBI	Silvi-Net: A dual-CNN (ResNet-18) approach	Classification

32	Tao et al., 2020	Subtropical	8.47	RGB	AlexNet & GoogLeNet	Object detection
33	Chiang et al., 2020	Temperate	NR	RGB	Mask R-CNN with transfer learning (ResNet-FPN backbone)	Instance segmentation
34	Briechle et al., 2020	Temperate	8.6	LiDAR + multispectral	3D deep neural network (DNN) PointNet++	Classification
35	Deng et al., 2020	Temperate	NR	RGB	Faster R-CNN	Object detection
36	Sylvain et al., 2019	Temperate	20	RGBI	VGG16S and ensemble learning	Classification
37	Fricker et al., 2019	Temperate	100	LiDAR + hyperspectral	CNN: 8 conv layers	Classification
38	Jiang et al., 2019	Temperate	20	CIR	FCN-DenseNet	Semantic segmentation



244

245 **Fig. 2.** Standing dead trees across biomes and spatial scales. (a) Field examples from boreal, temperate, and
 246 temperate forests. (b) Representation of standing dead trees in remote sensing imagery across spatial scales,
 247 from UAV imagery to Sentinel-2 observations. (c) Conceptual deep learning workflow for standing dead-tree
 248 detection and mapping. Image credits: boreal, Anwarul Chowdhury; temperate, Yan Cheng; tropical, Evan
 249 Gora.

250 **3 Remote sensing platforms and methodological advances in standing dead-tree** 251 **mapping**

252 **3.1 Advances in remote sensing platforms and data integration**

253 The reviewed literature shows that standing dead-tree mapping has been conducted using UAV, crewed aircraft,
254 and satellite platforms, with clear differences in spatial resolution, spatial extent, and analytical purpose (Fig.
255 3). Most studies relied on high-resolution optical imagery for crown- or tree-level detection, with 42.1% (16)
256 using RGB imagery only and 34.2% (13) using extended optical data such as RGBI, CIR, or red-edge bands. In
257 contrast, LiDAR-integrated approaches accounted for 15.8% (6) of the reviewed studies, while multispectral or
258 hyperspectral data without LiDAR represented 7.9% (3) (Fig. 3a). Most studies also relied on fine spatial
259 resolution, with 42.1% (16) using data in the 10–25 cm range, 15.8% (6) using imagery finer than 5 cm, and
260 10.5% (4) using imagery in the 5–10 cm range (Fig. 3a). Taken together, these patterns indicate that the
261 reviewed literature is centered primarily on high-resolution aerial image analysis, whereas broader-scale
262 satellite observations appear mainly in complementary or upscaling contexts.

263 Until recently, detecting and mapping standing dead trees beyond small scales was constrained by limited
264 scalability and insufficient automated processing over large areas. Only in the last decade has the convergence
265 of fine spatial resolution, frequent revisit capability, and efficient large-scale data processing made broader and
266 more automated standing dead-tree monitoring increasingly feasible. Advances in miniaturized sensors, high-
267 performance computing, and AI-driven image analysis have now enabled forest monitoring at resolutions
268 previously achievable only through field surveys (Lines et al., 2022; Schiefer et al., 2025; Xu and Jiang, 2025).
269 Modern UAVs can collect imagery with ground sampling distances down to approximately 1 cm, capturing fine
270 details such as crown structure, branch exposure, and canopy gaps. UAVs are particularly advantageous for
271 small to medium-sized monitoring areas, offering flexibility, low-cost, and the possibility of repeated temporal
272 surveys (Manfreda et al., 2018). UAV-based remote sensing commonly captures RGB, multispectral,
273 hyperspectral, and LiDAR data. LiDAR has been extensively employed for detecting standing dead trees
274 (Briechle et al., 2021; Polvivaara et al., 2024). However, its performance may decline when identifying small,
275 densely branched, or partially occluded targets (Miltiadou et al., 2018). At an intermediate scale, crewed
276 airborne platforms equipped with high-resolution digital cameras, multispectral sensors, or LiDAR complement
277 UAV surveys by extending coverage to thousands of hectares while retaining fine spatial detail. At broader
278 regional to continental scales, satellite remote sensing provides the widest spatial coverage and the most
279 consistent temporal observations. Very high-resolution commercial satellites such as WorldView-3 and SkySat
280 provide sub-meter imagery, while systems such as PlanetScope offer frequent revisit times for repeated
281 monitoring over large areas (Baldin and Casella, 2024; Liu et al., 2021; Shields et al., 2025). In addition, medium-
282 resolution missions such as Sentinel-2 and Landsat, although coarser in spatial resolution, provide regular
283 revisit schedules and dense time series that can partly offset this limitation by improving the detection of
284 standing dead tree dynamics through time. In the broader tree-mortality remote sensing literature, Ni et al.
285 (2025) reported that satellite-based data dominate previous studies, with optical imagery accounting for most
286 applications. This contrasts with the deep-learning-based standing dead-tree studies reviewed here, which are
287 more strongly centered on high-resolution UAV and airborne imagery.

288 The different remote sensing platforms are better understood as components of a multi-scale monitoring
289 framework that supports distinct use cases. UAVs are particularly valuable for local assessments, where very
290 high spatial resolution is needed to characterize fine-scale standing dead tree patterns. In other cases, local
291 UAV-based assessments are used as reference information for model development, calibration, and validation,
292 and are subsequently linked to airborne or satellite observations to support upscaling to broader areas. By
293 contrast, studies focused on regional to continental standing dead tree patterns typically rely on airborne
294 surveys, satellite observations, or upscaled products derived from these data sources. In this context,
295 combinations such as crewed aircraft or satellite optical imagery with UAV optical or UAV LiDAR data are better
296 understood as cross-scale integration for calibration, validation, and upscaling, rather than sensor fusion. UAVs
297 are therefore not typically used as a standalone source for wall-to-wall large-scale monitoring but instead
298 provide high-resolution reference data that can improve broader-scale standing dead-tree mapping products.

299 Moreover, standing dead-tree detection can benefit from integrating optical, spectral, and structural
300 information, although the relative importance of each data source depends not only on the specific objective
301 (e.g., presence detection versus structural quantification) but also on forest type, biome, canopy complexity,
302 and tree growth form. Each sensor type contributes complementary insights:

- 303 • Optical sensors capture visible and near-infrared reflectance, revealing changes in color and texture
304 associated with chlorophyll degradation or defoliation (Catalão et al., 2022; Liu et al., 2021; Ni et al.,
305 2025).
- 306 • Multispectral and hyperspectral sensors measure narrow spectral bands related to pigment status,
307 moisture conditions, and stress responses (Bergmüller and Vanderwel, 2022; Campbell et al., 2020;
308 Cotrozzi, 2022; Jutras-Perreault et al., 2023). Their usefulness for standing dead-tree detection depends
309 on the specific application as well as forest type, canopy structure, and operational scale. In particular,
310 while hyperspectral data may help identify subtle physiological differences, their broader operational
311 use for large-scale standing dead-tree monitoring remains limited by calibration requirements and
312 large data volumes.
- 313 • LiDAR provides three-dimensional structure, enabling the estimation of canopy height, crown volume,
314 and gap formation. This level of detail is particularly valuable for identifying standing dead trees that
315 are partially obscured by overlapping crowns (Korpela et al., 2023; Krzystek et al., 2020; Kuzmin et al.,
316 2026; Miltiadou et al., 2020). High-resolution photogrammetric point clouds can also recover tree
317 structural attributes when image overlap, spatial resolution, and canopy conditions are favorable,
318 although LiDAR is generally more robust in dense or structurally complex forests due to its capability
319 to penetrate the upper canopy layers (Filippelli et al., 2019; McNicol et al., 2021; White et al., 2013).

320 Overall, integrating these datasets, often referred to as sensor fusion, can produce synergistic improvements
321 in detection accuracy. Fusion can occur at multiple levels, including the data and feature levels. Combination
322 approaches integrating LiDAR and optical data have shown strong potential for improving standing dead-tree
323 detection, although results are not directly comparable across studies because they depend on dataset
324 characteristics and evaluation metrics (Briechle et al., 2020; see also Section 6). As sensor technology becomes
325 more accessible, such integrative frameworks are expected to become standard practice.

326

327 **3.2 From visual interpretation to deep learning automation**

328 Early approaches to standing dead-tree mapping relied either on field-plot measurements linked with remotely
329 sensed data to extrapolate standing dead tree patterns or on manual and semi-automatic interpretation of
330 aerial imagery, where analysts visually identified discolored or defoliated crowns (International Tree Mortality
331 Network, 2025; Polewski et al., 2015a). While plot-based approaches provided reliable ground information,
332 they were limited by sparse sampling and scaling uncertainties, whereas visual interpretation of imagery,
333 although effective at small scales, was labor-intensive and prone to observer bias (International Tree Mortality
334 Network, 2025; Wulder et al., 2012). The introduction of machine learning marked an initial step toward
335 automated image-based detection by incorporating spectral indices (e.g., NDVI, NBR) and textural metrics into
336 classifiers such as Random Forest and Support Vector Machines. However, these approaches depended heavily
337 on handcrafted feature engineering and often struggled to generalize across forest types and environmental
338 conditions (Sheykhmousa et al., 2020).

339 The transition to deep learning substantially advanced automated standing dead-tree mapping. By learning
340 hierarchical spatial and spectral representations directly from imagery, deep learning models reduce reliance
341 on manual feature design and enable more robust detection of crown discoloration, defoliation, and structural
342 degradation (Chowdhury et al., 2025; Weinstein et al., 2019). Numerous recent studies have applied deep
343 learning methods to detect standing dead trees in UAV and airborne imagery (Jiang et al., 2023; Joshi and
344 Witharana, 2025; Junttila et al., 2024; Lucas et al., 2024; Möhring et al., 2025; Schiefer et al., 2023; Schwarz et
345 al., 2024; Yao et al., 2024; Zhang et al., 2025a; Zhou et al., 2024). Furthermore, transfer learning and domain
346 adaptation strategies enhance model portability across regions and forest types, improving the potential for
347 scalable monitoring of standing dead trees (see Section 4.3). Detailed comparisons of specific architectures and
348 their performance characteristics are discussed in Section 4.

349 **3.3 Validation practices and the role of field observations**

351 Validation remains an underdeveloped aspect of standing dead-tree mapping. Most reviewed studies assessed
352 performance using manually annotated imagery or withheld image tiles from the same remotely sensed
353 dataset. Although such approaches are useful for evaluating agreement with expert interpretation, they do not
354 fully establish whether mapped standing dead trees correspond to standing dead trees actually present in the
355 field. Only a limited number of studies incorporated field observations into validation, either directly or in
356 combination with image-based reference data (Table A2). Examples include Mäyrä et al. (2025), who compared
357 UAV-interpreted deadwood with field-measured deadwood; Matejčíková et al. (2024), who used a ground-truth
358 dataset produced with partial field verification; and Fricker et al. (2019), who linked field-based tree
359 observations to manually delineated image labels used for training and testing. Together, these studies show
360 that field data can reveal omission and visibility biases that are not captured by image-based validation alone.

361

362 4 Model architectures and performance patterns in standing dead-tree detection

363 Deep learning has become increasingly important in remote-sensing-based standing dead-tree detection.
 364 Among the reviewed studies, object detection approaches were the most common category (39.5%), followed
 365 by CNN-based classification models (23.7%), hybrid or ensemble methods (15.8%), FCN/U-Net architectures
 366 (13.2%), and vision transformer-based models (7.9%) (Fig. 3a). In addition, more than two-thirds of the
 367 reviewed studies were conducted in temperate biomes (Fig. 3a). However, these model categories are not
 368 always directly comparable because they often target different outputs, including patch-level classification,
 369 pixel-wise segmentation, crown-level localization, instance segmentation, and sub-pixel mapping. Reported
 370 performance also depends strongly on forest structure, sensor modality, spatial resolution, annotation quality,
 371 evaluation protocol, and pre- or post-processing choices. Therefore, differences among model families should
 372 be interpreted as descriptive patterns rather than direct evidence of superiority across studies.

373 4.1 Deep learning architectures for standing dead-tree detection

375 **Table 2.** Overview of deep learning architectures used for standing dead-tree detection, including their main
 376 advantages, limitations, typical applications, and input-data flexibility reported in the literature.

Architecture	Main advantages	Key limitations	Use	Input data & flexibility
CNNs	Capture localized spectral and textural features; effective for crown-level classification; adaptable to high-resolution UAV imagery	Limited global context; patch-based approaches reduce spatial precision; sensitive to training data quality	Crown-level classification; localized mortality signals; well-represented training data	Flexible with raster inputs beyond RGB, including multispectral, hyperspectral, LiDAR-derived layers, and temporal stacks.
FCN / U-Net	Pixel-wise segmentation with accurate boundary delineation; preserves spatial detail; effective in complex canopies	Requires large, high-quality annotated datasets; weaker performance in sparse mortality conditions	Dense canopy segmentation; precise crown delineation; boundary-sensitive tasks	Accept arbitrary multi-channel raster inputs and are widely used with multispectral, RGBI, and temporal data.
Object detection	Instance-level detection; high recall; effective for counting and mapping individual trees; strong performance in recent YOLO variants	Limited boundary precision; challenges with overlapping crowns in dense canopies	Individual tree detection and counting; sparse or patchy mortality; operational mapping	Most often applied to RGB/RGBI imagery; multi-channel use is possible but less common and usually requires adaptation.
Hybrid / Ensemble	Combines complementary model strengths;	High computational	Heterogeneous forests; complex	Most flexible; can combine imagery,

	improved robustness in complex environments; integrates spatial and structural information	cost; complex workflows; potential error propagation between stages; results often study-specific	canopy structures; multi-stage detection and delineation	structural data, and temporal information across stages.
Vision transformers	Capture global context and long-range dependencies; robust in heterogeneous and mixed-species conditions	High data and computational requirements; less efficient for small datasets	Mixed-species forests; large-scale heterogeneous datasets; complex spatial patterns	Support multi-channel and multi-temporal inputs but usually need more data and computation.

377

378 4.1.1 Convolutional neural networks (CNNs)

379 CNNs formed an early foundation for crown- or patch-level standing dead-tree classification, where the goal is
380 to label crowns or image patches as dead, damaged, or alive (Schwenke et al., 2025). CNNs are well suited to
381 this task because they capture localized spatial and spectral patterns associated with tree mortality, such as
382 crown discoloration, thinning, or structural collapse. Early applications using standard architectures such as
383 AlexNet and GoogLeNet demonstrated the feasibility of CNN-based standing dead-tree detection, while also
384 highlighting limitations related to feature representation and dataset constraints (Tao et al., 2020). Subsequent
385 studies have shown that performance can benefit from architectures tailored to the characteristics of domain-
386 specific imagery rather than simply increasing model depth. For example, lightweight or shallow CNNs have
387 been successfully applied to high-resolution UAV imagery, suggesting that carefully optimized models may be
388 particularly suitable for crown-focused detection tasks (Khatri-Chhetri et al., 2024; Wong et al., 2024).
389 Incorporating temporal information can further enhance detection: Dixon et al. (2023) developed a 3D spatio-
390 temporal CNN that integrates multi-date imagery to track gradual crown deterioration, highlighting the value
391 of temporal feature learning for long-term forest monitoring. Hybrid CNN designs extend applicability to more
392 challenging environments. Silvi-Net (Briechle et al., 2021), a dual-stream CNN, improves robustness in mixed-
393 species forests by handling variability in crown shape and spectral characteristics. Similarly, Fricker et al. (2019)
394 showed that an 8-layer CNN reliably distinguishes healthy and dead crowns across diverse forest types (F1-
395 score 0.87).

396 Despite their strengths, standard CNN classifiers can be limited by restricted receptive fields, which may reduce
397 their ability to incorporate broader spatial context. In patch-based frameworks, predictions are made at the
398 patch level, assigning a single label per tile and thereby limiting spatial localization and precise crown
399 delineation. While fully convolutional segmentation architectures address this through dense pixel-wise
400 predictions, CNN-based approaches remain highly dependent on high-quality training data and may
401 underperform in dense mixed forests without domain-specific tuning. Overall, CNNs are most suitable for
402 crown- or patch-level classification when mortality signals are localized and well represented in the training
403 data, whereas they are less suitable for dense-canopy segmentation or instance-level mapping requiring
404 precise crown boundaries.

405

406 **4.1.2 Fully convolutional networks (FCNs) and U-Net derivatives**

407 Fully Convolutional Networks (FCNs), particularly U-Net and its variants, are widely used for pixel-wise standing
408 dead tree crown segmentation because their encoder–decoder architecture with skip connections preserves
409 spatial detail and enables precise localization (Long et al., 2014; Ronneberger et al., 2015). This makes them
410 well suited to delineating crown boundaries and capturing subtle spectral and structural characteristics in
411 dense or complex canopies. Enhanced U-Net architectures, such as those incorporating atrous spatial pyramid
412 pooling and inverted residual blocks (Junttila et al., 2024) achieve F1-scores of up to 0.93, demonstrating
413 improved multi-scale feature extraction, boundary precision, and robustness against shadows or
414 heterogeneous canopy structures.

415 Attention mechanisms and post-processing further enhance performance. The TreeMort-3T-UNet (Rahman et
416 al., 2025) combines self-attention with watershed filtering to isolate standing dead crowns in overlapping
417 canopies, achieving an F1-score of 0.59, highlighting its ability to address structural complexity despite lower
418 overall accuracy. Lightweight models like EfficientUNet++ (Schwarz et al., 2024) maintain segmentation quality
419 while improving computational efficiency. FCNs have limitations in sparse-mortality settings, where isolated
420 standing dead trees occupy few pixels; their sensitivity to local context can cause missed detections or false
421 positives. Performance also depends on high-quality, large-scale annotated datasets, as inconsistent or limited
422 labels reduce generalization. Overall, U-Net and FCN derivatives are particularly useful for dense-canopy
423 segmentation, benefiting from boundary-preserving skip connections, multi-scale feature learning, and
424 attention/post-processing enhancements.

425

426 **4.1.3 Object detection frameworks**

427 Object detection frameworks have become popular for standing dead-tree detection, particularly for
428 identifying and counting individual trees. Unlike CNN classifiers or FCNs, these models generate bounding boxes
429 or instance masks, allowing them to isolate discrete crowns—a key advantage in sparse-mortality or dense
430 mixed forests. YOLO-based models are prominent in recent studies due to their real-time performance and high
431 detection accuracy. For example, Yang et al. (2025) enhanced YOLOv5 with SE attention, BiFPN, and EIoU loss,
432 achieving an F1-score of 0.83, while Zhou et al. (2024) improved YOLOv7 with SimAM and WIoU optimization,
433 reaching 0.94. Zhang et al. (2025a) developed YOLOv9-ECA, integrating Efficient Channel Attention, and
434 reported one of the highest F1-scores among the reviewed local case studies. These studies demonstrate that
435 attention mechanisms and multi-scale feature fusion enable object detectors to capture subtle spectral and
436 structural cues associated with standing dead trees. Lightweight variants, such as YOLOv4 with a MobileNetV3
437 backbone (Jin et al., 2023, F1-score 0.97) and LDS-YOLO (Wang et al., 2022), further show that high accuracy
438 can be maintained while reducing computational cost, supporting operational UAV-based mapping.

439 Mask R-CNN is widely used when instance segmentation and detailed crown geometry are required, whereas
440 Faster R-CNN is more suitable for bounding-box-based object localization. Lucas et al. (2024) reported an F1-
441 score of 0.91 using Mask R-CNN with a ResNet-50 backbone, while Yao et al. (2024) achieved 0.71. Although
442 slower than YOLO, these models provide precise crown shapes useful for biomass estimation and crown-level
443 analysis. Object detectors often report strong performance in sparse or patchy mortality conditions, particularly

444 where the objective is to localize and count individual dead crowns. However, in dense-canopy forests,
445 overlapping crowns can challenge bounding-box precision, making FCNs or U-Net derivatives more effective for
446 boundary-sensitive segmentation. Overall, the choice of detection framework should consider forest structure,
447 standing dead-tree distribution, annotation format, and mapping objective. YOLO-based models are well suited
448 to rapid localization and counting, whereas Mask R-CNN and related instance-segmentation models are
449 preferable when crown geometry is important.

450

451 **4.1.4 Hybrid and ensemble models**

452 In this review, hybrid models refer specifically to approaches that combine two or more model architectures or
453 processing stages within a single detection workflow, rather than to the combination of different data sources
454 or sensors. Ensemble models refer to approaches that combine predictions from multiple models to improve
455 robustness. Hybrid and ensemble architectures combine the strengths of multiple deep learning models,
456 enabling simultaneous modeling of local textures, global context, and temporal dynamics, which are critical in
457 forests with complex mortality patterns or highly variable canopy structures. For example, TreeMort-3T-UNet
458 (Rahman et al., 2025) represents an architecture-level hybrid workflow that integrates a self-attention U-Net
459 with multi-stage post-processing, including watershed and adaptive filtering. Related multi-stage workflows,
460 such as the EfficientUNet and deep watershed approach of Cheng et al. (2024), similarly aim to improve
461 instance separation in dense or overlapping canopies. These hybrid workflows address common FCN limitations
462 by incorporating structural priors, which are essential for precise counting and delineation of standing dead
463 trees.

464 Another common hybrid strategy combines object detection and segmentation in multi-stage pipelines. YOLO
465 or Mask R-CNN models first localize potential standing dead tree crowns, followed by U-Net variants or deep
466 watershed algorithms to refine boundaries. This strategy can outperform standalone models in some case
467 studies, although gains are workflow- and dataset-dependent. Ensemble approaches can further improve
468 robustness by aggregating predictions from multiple models or repeated realizations of the same model; for
469 example, Sylvain et al. (2019) combined predictions from multiple CNN runs with different random
470 initializations to reduce random variation and produce smoother dead forest cover maps. In contrast, methods
471 such as ADA-Net (Ahishali et al., 2025) are better characterized as domain-adaptation frameworks rather than
472 ensemble models, as they are designed to improve transferability across varying forest types or sensor
473 conditions.

474 However, these methods come with trade-offs: they are computationally intensive, require larger datasets and
475 model parameters, and may propagate errors between stages if initial detection fails. Overall, hybrid and
476 ensemble models are particularly relevant for heterogeneous forests and complex canopy conditions, although
477 their reported advantages are often study-specific and should therefore be interpreted cautiously across
478 different datasets and evaluation settings (Zhao et al., 2023).

479

480 **4.1.5 Vision transformer-based models**

481 Vision Transformers (ViTs) and transformer-based hybrids have recently emerged as promising alternatives to
482 CNNs for standing dead-tree detection, largely due to their global self-attention mechanisms, which capture
483 long-range dependencies and contextual relationships across entire images. Unlike CNNs, whose receptive
484 fields are limited, ViTs can help capture subtle variations in crown coloration, texture, or structure that may be
485 overlooked by conventional models. SegFormer-based architectures may offer advantages under variable
486 illumination and mixed-species conditions, effectively distinguishing healthy from unhealthy crowns over large
487 spatial extents (Joshi and Witharana, 2025). Hybrid designs, such as SegFormer-B5 combined with a U-Net
488 decoder, leverage transformer feature extraction while preserving fine-grained crown boundaries, achieving
489 competitive F1-scores (~ 0.71 ; Möhring et al., 2025).

490 Transformer-CNN hybrids, particularly those incorporating Swin-Transformer backbones, may also improve
491 detection performance in object detection workflows. Jiang et al. (2023) reported an F1-score of 0.94 using a
492 Swin-Transformer backbone with Faster R-CNN, suggesting that transformer-based feature extraction can
493 support robust crown-level localization. Beyond standing dead-tree detection, transformer models have shown
494 strong potential in broader remote sensing applications (Wang et al., 2024). However, ViTs generally require
495 larger training datasets and higher computational resources than many CNN-based models, which can limit
496 their operational use in small annotated datasets. Overall, transformer-based models are promising, but their
497 advantages for standing dead-tree detection should be evaluated more rigorously using shared benchmarks,
498 cross-site validation, and multi-sensor datasets.

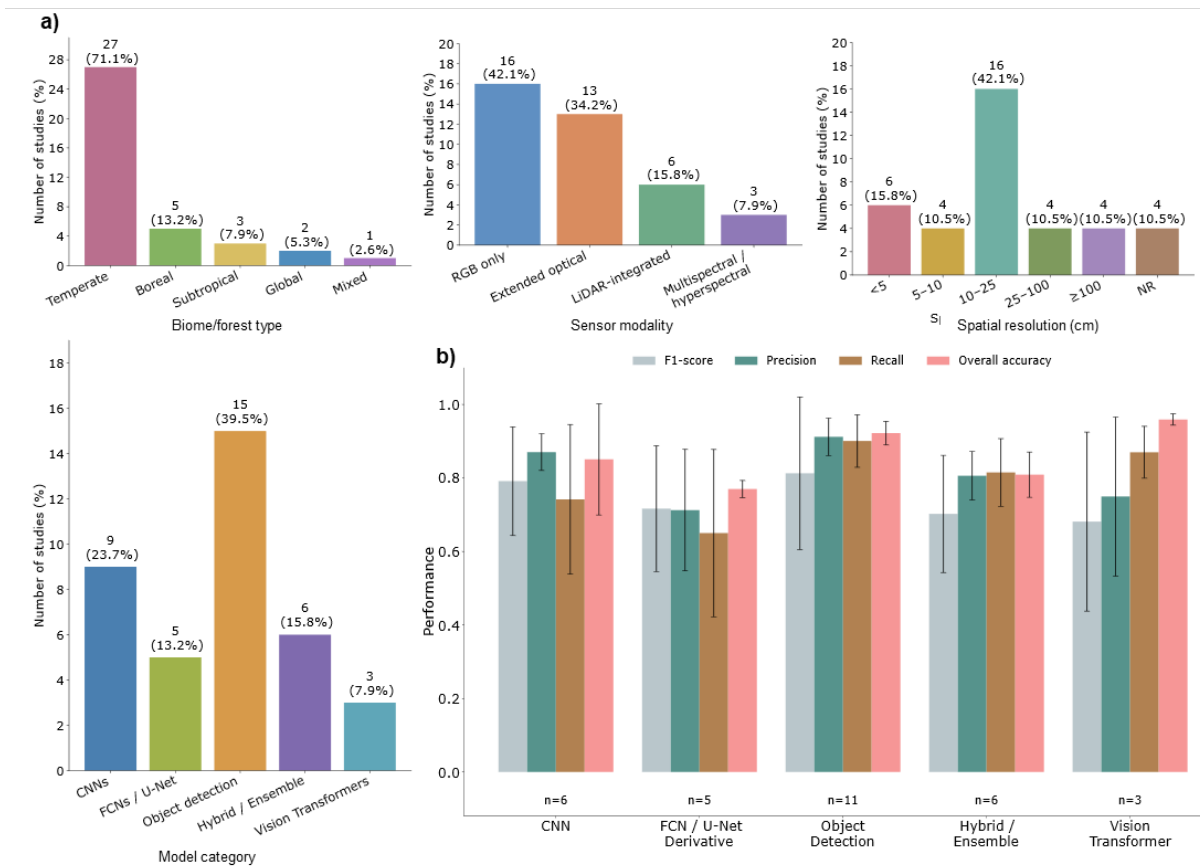
499 Our analysis included 31 studies that reported comparable quantitative metrics, including F1-score, precision,
500 recall, or overall accuracy (Fig. 3b). Because these metrics were extracted from heterogeneous studies rather
501 than a common benchmark, they should be interpreted as descriptive summaries rather than direct evidence
502 of superiority among model families. Across model categories, reported mean F1-scores ranged from 0.68 to
503 0.81, precision from 0.71 to 0.91, recall from 0.65 to 0.90, and overall accuracy from 0.77 to 0.96. Object
504 detection models showed high mean values across several metrics, while transformer-based models showed
505 the highest mean overall accuracy. However, these patterns should be interpreted cautiously because studies
506 differed in sensor modality, spatial resolution, forest type, annotation protocol, validation design, and task
507 definition. Standardized benchmark datasets and shared evaluation protocols are therefore needed before
508 robust conclusions can be drawn about the relative performance of different model families.

Box 1. Key synthesis findings from the reviewed literature

- Most reviewed studies rely on high-resolution RGB or RGBI UAV/airborne imagery.
- Object detection models are most common for individual-tree localization and counting.
- U-Net-type architectures are widely used for semantic segmentation of dead crowns or canopy mortality.
- Field validation remains rare; most studies rely on image interpretation.
- Cross-biome and cross-sensor transferability remains weakly demonstrated.
- Standardized benchmark datasets are the most urgent requirement for robust model comparison.

509

510



511

512 **Fig. 3.** Overview of the reviewed studies and model performance across deep learning categories.
 513 a) Distribution of the total number of reviewed studies ($n = 38$) according to biome/forest type,
 514 spatial resolution, and model category. b) Performance comparison across model categories based on studies
 515 that reported quantitative metrics ($n = 31$), showing mean F1-score, precision, recall, and overall accuracy; error

516 bars indicate variability (standard deviation) across studies, and n denotes the number of publications per
517 category.

518 **4.2 Factors influencing model accuracy**

519 Model performance depends not only on architecture but also on data characteristics, preprocessing, post-
520 processing, and evaluation design.

521

522 **4.2.1 Data-related factors: resolution, training size, and annotation quality**

523 Model performance in standing dead-tree detection is fundamentally constrained by data characteristics.
524 Resolution across spatial, spectral, and temporal dimensions, together with dataset size and diversity, and
525 annotation quality influence not only what a model can learn, but also how reliably its performance can be
526 evaluated. These factors therefore determine both predictive capacity and the extent to which model
527 performance can be validly demonstrated. If indicators of death are not visible at the available resolution, or if
528 annotations are weak, inconsistent, or incomplete, neither training nor evaluation can fully capture true model
529 capability. The following sections examine how spatial detail, dataset composition, and annotation design
530 jointly influence model generalization, error patterns, and the validity of reported results across forest
531 conditions.

532 ***Resolution***

533 Spatial resolution determines how clearly diagnostically relevant canopy features are represented in the
534 imagery and therefore directly influences the detectability of standing dead trees. High-resolution UAV or
535 airborne imagery can capture fine-scale characteristics such as crown boundaries, branch structure, canopy
536 gaps, and partial defoliation, all of which are important indicators of tree death (Matejčiková et al., 2024). In
537 contrast, coarser imagery may obscure small, partially occluded, or early-stage standing dead trees, thereby
538 reducing detection sensitivity. While reported ground sampling distances (GSD) have varied from centimeter-
539 level to several meters (Fig. 3a), GSDs of approximately 4–8 cm have been reported as effective for standing
540 dead tree segmentation in some contexts, although no universally optimal resolution can yet be identified
541 (Möhring et al., 2025). In general, finer spatial resolution improves the visibility of crown-level indicators
542 relevant to standing dead-tree detection. However, the benefits of very high-resolution imagery are
543 constrained by the reduced spatial context that can be processed within computationally feasible image
544 patches. Higher spatial resolution often necessitates smaller patches, which can limit the contextual
545 information available to the model even when fine-scale features are well resolved (Kattenborn et al., 2021;
546 Möhring et al., 2025; Schiefer et al., 2020). As discussed in Section 3.1, spectral resolution provides
547 complementary information by capturing differences in reflectance related to canopy condition, including
548 pigment degradation and moisture status, which can support the detection of standing dead trees beyond what
549 is visible from structural features alone. Temporal resolution further influences detectability by determining
550 whether the progression of tree mortality can be observed. Standing dead trees may transition through
551 multiple stages, and their detectability can depend on the timing of image acquisition. Multi-temporal
552 observations can improve detection by capturing change dynamics, such as gradual decline or sudden canopy
553 loss, and by helping to distinguish mortality from seasonal or short-term variability (Dixon et al., 2023).

554 However, temporal data are often limited by acquisition frequency, consistency, and challenges related to co-
555 registration and phenological variation, and many studies therefore rely on single-date imagery.

556 ***Training size and dataset diversity***

557 Beyond resolution, dataset size and heterogeneity strongly influence model generalization. In computer vision,
558 stable performance often requires on the order of 10^3 – 10^4 annotated instances per class, depending on model
559 complexity (Krizhevsky et al., 2012). However, ecological applications typically operate with far fewer samples
560 (e.g., 150–1000 instances per class), making dataset diversity across sites, species composition, canopy
561 structure, illumination, and phenological stages particularly important for improving transferability (Shahinfar
562 et al., 2020). Large-scale initiatives, such as the 100-million-crown dataset by Weinstein et al. (2021),
563 demonstrate clear performance gains when models are trained on extensive and heterogeneous annotations.

564 However, standing dead tree occurrences are typically rare, leading to pronounced class imbalance. Limited
565 representation of standing dead trees biases models toward the dominant healthy class and increases omission
566 errors. Expanding annotated samples through multi-site data collection, targeted sampling of standing dead
567 tree cases, or synthetic augmentation can improve detection performance (Khatri-Chhetri et al., 2024). High-
568 capacity architectures such as Mask R-CNN, U-Net variants, and transformer-based models particularly depend
569 on sufficient data diversity to avoid amplifying site-specific biases.

570 ***Annotation quality and format***

571 Data quantity alone does not ensure reliability, but robust standing dead-tree detection does not necessarily
572 require precise or complete manual labels (Weinstein et al., 2019). In practice, crown-level annotation often
573 does not scale across large and heterogeneous forest settings (Wang et al., 2026). Although inaccurate
574 delineations, misclassified standing dead trees, and omission of small or partially dead trees can introduce label
575 noise, recent AI frameworks increasingly address these limitations directly. Weakly supervised learning, semi-
576 supervised learning, active learning, and human-in-the-loop refinement can work with incomplete, noisy, or
577 weak labels while reducing annotation effort (Polewski et al., 2015a; Weinstein et al., 2019). Annotation quality
578 therefore remains important, but not as an absolute prerequisite for effective modeling. Rather, reliable
579 performance depends on how well the annotation strategy matches the model architecture, learning
580 framework, and forest structure. Instance segmentation networks generally benefit from precise crown
581 polygons, whereas detection-oriented models may work effectively with weaker supervision such as bounding
582 boxes, centroids, points, or coarse labels (Zhao et al., 2023). Automatic and semi-automatic annotation
583 methods can further support scalable dataset generation and iterative improvement (Wang et al., 2026). As
584 Steier et al. (2024) show, annotation errors can still distort training signals and ecological inference, so
585 uncertainty must be managed explicitly. Overall, reliable performance depends less on label perfection alone
586 than on the compatibility among annotation strategy, learning framework, model type, and forest structure.

587 588 **4.2.2 Pre-processing: ensuring spectral consistency and training robustness**

589 Pre-processing prepares remote-sensing imagery for model training by standardizing data where necessary,
590 organizing it into usable inputs, and introducing transformations that improve generalization (Sani-Mohammed
591 et al., 2022; Weinstein et al., 2019). In standing dead-tree detection, model performance does not depend on

592 spectral information alone, but may instead rely on a combination of spectral, textural, structural, and
593 contextual cues (Möhring et al., 2025; Zhao et al., 2023). Accordingly, pre-processing should not be understood
594 simply as preserving radiometric fidelity, but as balancing input consistency with sufficient variability to reduce
595 overfitting across different acquisition and forest conditions (Han et al., 2022).

596 The relevance of radiometric correction depends on sensor type, acquisition workflow, and modelling
597 objective. While normalization or calibration can improve comparability between images acquired under
598 different conditions, exact spectral fidelity is not always critical in high-resolution UAV-based standing dead-
599 tree detection, where texture, crown shape, branching structure, and local canopy context may be equally or
600 more informative (Schiefer et al., 2023). Accordingly, many workflows deliberately introduce spectral variability
601 during training through augmentations such as brightness or contrast in order to improve robustness to
602 changing acquisition conditions (Han et al., 2022; Sani-Mohammed et al., 2022).

603 Geometric pre-processing is mainly relevant where spatial distortions or misalignment affect crown
604 representation, annotation accuracy, or the integration of auxiliary layers. Orthorectification and co-registration
605 can improve alignment between imagery, labels, and additional data sources, whereas misregistration may shift
606 crown boundaries and introduce training noise. At the same time, geometric variability is often introduced
607 deliberately through augmentations such as rotation, flipping, and patch shifts to improve robustness and
608 reduce overfitting (Sani-Mohammed et al., 2022; Yao et al., 2024), with rotation and flipping being the most
609 frequently reported augmentation strategies in previous studies (Fig. A1).

610 Pre-processing also includes tiling, patch extraction, and sampling design. Tiling large orthomosaics into smaller
611 patches improves computational feasibility, but patch size must preserve crown integrity and sufficient spatial
612 context while avoiding boundary artefacts (Han et al., 2022; Polewski et al., 2015b; Schiefer et al., 2023).
613 Because standing dead trees are often rare, pre-processing workflows must also address class imbalance.
614 Oversampling minority-class patches, targeted patch selection, weighted loss functions, and synthetic
615 augmentation or copy-paste strategies can reduce bias toward the dominant healthy class and improve
616 sensitivity to standing dead tree occurrences (Han et al., 2022; Zhou et al., 2024).

617 Finally, pre-processing may include the integration of complementary structural information, such as canopy
618 height data or digital surface models (DSMs), to enrich feature representation beyond spectral imagery alone.
619 Such auxiliary layers can improve discrimination between dead and healthy crowns, especially where structural
620 differences are more consistent than spectral responses (Yao et al., 2024).

621 622 **4.2.3 Post-processing: refining ecological realism and boundary precision**

623 While deep learning models generate increasingly accurate pixel- or object-level predictions, their raw outputs
624 often require refinement to achieve ecologically realistic crown delineations. Post-processing techniques
625 therefore play a complementary role in improving boundary precision, reducing false positives, and enforcing
626 geometrically plausible crown structures. Broadly, these approaches aim to shift predictions from purely data-
627 driven segmentation toward structurally coherent tree representations. However, post-processing parameters
628 should be reported transparently because thresholding, filtering, and watershed settings can substantially
629 affect omission and commission errors.

630 ***Shape-constrained refinement***

631 One class of post-processing methods incorporates explicit shape constraints to regularize crown geometry. For
632 example, Shelton et al. (2021) combine model-derived probability maps with an active contour (level set)
633 framework, in which contours evolve by minimizing an energy function that balances image-based likelihoods
634 with smoothness and shape priors. This approach reduces irregular boundaries and regularizes crown
635 geometry, particularly in heterogeneous canopy conditions. Similarly, Polewski et al. (2020) integrate
636 generative adversarial network (GAN)-based shape priors into the segmentation process, constraining
637 predicted crowns to a learned manifold of realistic tree geometries. By embedding structural expectations
638 directly into refinement, such approaches mitigate spurious shapes that arise from local spectral noise or
639 canopy overlap. These methods highlight an important conceptual shift: rather than relying solely on pixel-wise
640 confidence, segmentation is guided by ecological knowledge of crown morphology.

641 ***Instance-boundary refinement***

642 Another widely used strategy focuses on improving separation between adjacent crowns. Watershed
643 segmentation is often applied in a marker-controlled manner and has proven effective in refining instance
644 boundaries and reducing crown merging. In a recent dual-task U-Net framework, Rahman et al. (2025) apply
645 watershed post-processing combined with adaptive filtering to reduce over-segmentation and suppress false
646 positives. Such approaches are particularly valuable in dense forests where crown overlaps complicate
647 instance-level detection.

648 ***Noise reduction and structural cleanup***

649 Morphological filtering operations, such as opening and closing, are commonly used to remove small, isolated
650 pixel clusters and smooth crown edges. Although comparatively simple, these operations can substantially
651 improve map readability and reduce artefactual detections, especially in high-resolution imagery where pixel-
652 level noise may propagate into fragmented predictions.

653

654 **4.3 Transfer learning and large-scale mapping**

655 Scaling standing dead-tree detection from localized UAV surveys to regional or global monitoring is challenged
656 by domain shift: systematic differences in spectral characteristics, sensor types, forest structure, and acquisition
657 conditions that reduce model transferability. Transfer learning can support scalability by initializing networks
658 with pretrained weights from large visual datasets (e.g., ImageNet), enabling stable, generalizable feature
659 representations that accelerate convergence, reduce annotation requirements, and improve performance
660 under limited data (Ma et al., 2024). By pre-training models on forest species classification, networks can learn
661 transferable representations that accelerate convergence when fine-tuned for standing dead-tree detection
662 (Rahman et al., 2025). Large-scale workflows typically follow a three-stage paradigm: broad pretraining,
663 localized fine-tuning with site-specific annotations, and lightweight domain adaptation to harmonize spectral
664 or seasonal differences, mirroring successful strategies in tree-crown delineation, forest-type classification, and
665 canopy-health assessment (Kattenborn et al., 2021).

666 Despite its advantages, transfer learning alone cannot fully overcome domain discrepancies. Integrating
667 domain adaptation methods, self-supervised representation learning, and few-shot approaches allows models

668 to align feature distributions across regions and leverage unlabeled imagery for scalable training (Ahishali et
669 al., 2025; Gevaert et al., 2025; Rahman et al., 2025). Open, standardized datasets such as [deadtrees.earth](#)
670 (Mosig et al., 2026b) further enhance model generalization by exposing networks to diverse forest types,
671 mortality stages, and disturbance gradients, while enabling benchmarking and reproducibility. Together, these
672 strategies could help shift standing dead-tree detection from site-specific modelling toward more transferable
673 and scalable mapping, paving the way for continuous, global forest health assessment with minimal
674 dependence on manual annotation.

675

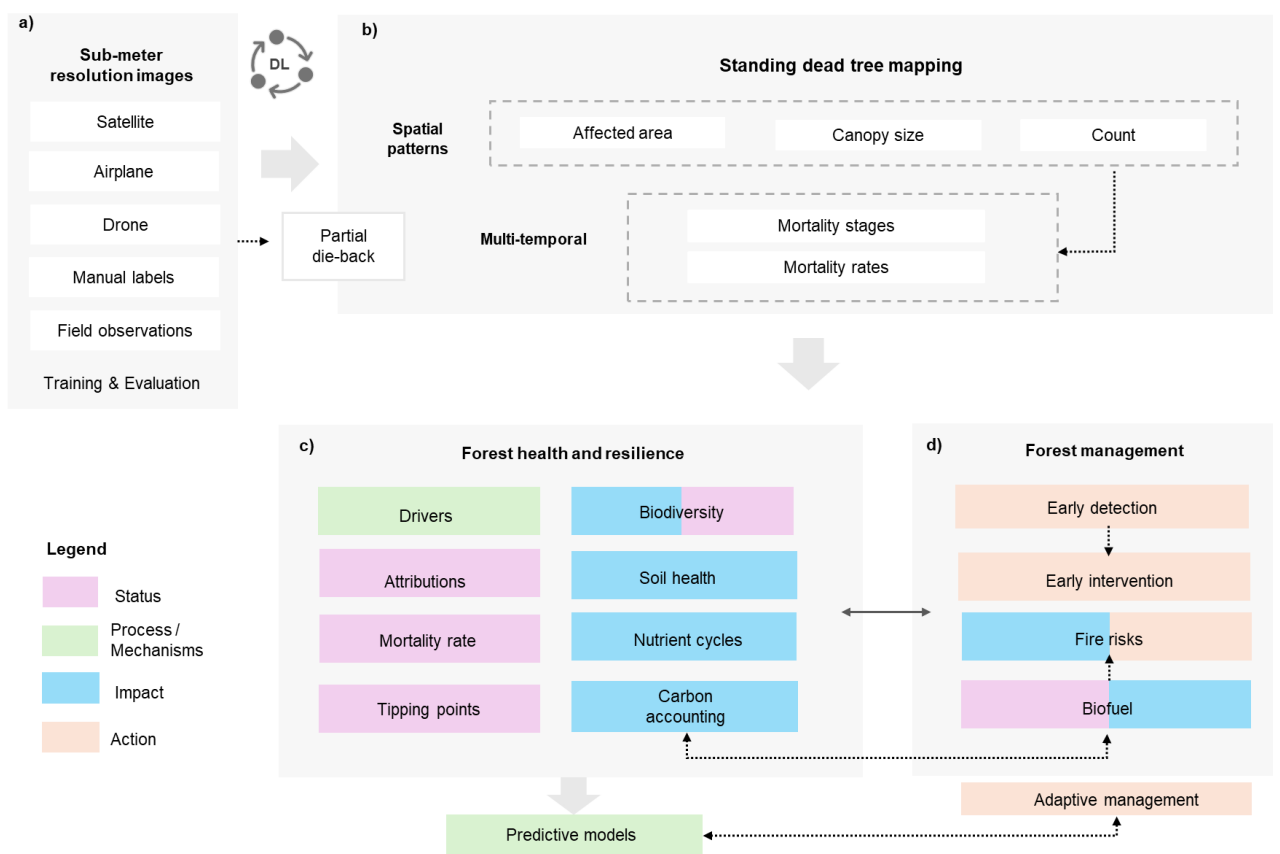
676 **5 Implications of standing dead-tree mapping**

677 The ability to map standing dead trees across extensive forest landscapes has substantially improved the
678 quantification of disturbance regimes and patterns of standing dead-tree occurrence. Traditional approaches
679 based on field plots or coarse-resolution satellite indices captured disturbance only at aggregated scales, often
680 obscuring fine-scale standing dead tree patterns driven by species-specific physiology, microsite variability, or
681 competition. Advances in high-resolution remote sensing and deep learning now enable tree-crown-level
682 detection across hundreds to thousands of hectares. For example, LiDAR- and multispectral-based assessments
683 revealed that more than 25% of trees in drought-exposed areas of the Sierra Nevada died between 2013 and
684 2017, with strong spatial clustering linked to elevation, water stress, and stand density (Hemming-Schroeder et
685 al., 2023). Similar improvements have been reported using fused LiDAR and multispectral data in Central
686 Europe (Krzystek et al., 2020; Liu et al., 2021) and UAV-based deep learning approaches (Rahman et al., 2025).
687 As shown in Fig. 4, these maps can provide metrics such as affected area, canopy size, mortality intensity, and
688 mortality rates. These spatially explicit standing dead tree data provide new insights into forest health,
689 resilience, and biogeochemical processes. Tree mortality represents a key transition in carbon cycling, shifting
690 biomass from live pools to necromass and influencing respiration, nutrient mineralization, and carbon turnover.
691 High-resolution standing dead-tree maps reduce uncertainty in deadwood pool initialization, particularly where
692 field data are limited, and remote sensing increasingly complements and extends ground monitoring for
693 representing carbon stock transitions (Bueno et al., 2025; Martinuzzi et al., 2009; Ni et al., 2025). Tree mortality
694 also alters transpiration, canopy interception, snow dynamics, albedo, and aerodynamic roughness, affecting
695 surface energy balance and evapotranspiration. Spatially explicit standing dead-tree maps further improve
696 attribution of carbon and water cycle anomalies by distinguishing acute disturbances from background
697 mortality (Senf and Seidl, 2021). These spatial products make the ecological functions of deadwood measurable
698 by quantifying standing dead-tree density, spatial configuration, and decay heterogeneity relevant to
699 biodiversity, including cavity-nesting birds, saproxylic insects, fungi, and microbial decomposers (Bujoczek et
700 al., 2021; Löfroth et al., 2023; Marchi et al., 2018; Seibold and Thorn, 2018; Seidling et al., 2014).

701 When integrated with multi-scale data and modelling approaches, standing dead-tree maps support prediction
702 and management of forest dynamics. While satellite time series capture large-scale disturbance patterns,
703 standing dead-tree maps provide the spatial detail needed to resolve local stand conditions. Combining these
704 datasets links standing dead-tree patterns to climatic drivers and landscape-scale disturbance regimes,
705 although interpretation still requires ancillary ecological and field data. Spatially explicit models show that
706 incorporating fine-scale standing dead tree patterns improves predictions of future die-off hotspots under

707 climate stress (Ganz et al., 2025). These insights support management applications including early detection of
 708 disturbances, intervention planning, wildfire risk assessment through fuel mapping, and adaptive management
 709 strategies (Bell et al., 2021; Cheng et al., 2024; Junttila et al., 2024; Mahanta et al., 2024; Schiller et al., 2024;
 710 Turkulainen et al., 2023). Standing dead-tree mapping also supports policy frameworks such as the EU
 711 Biodiversity Strategy and REDD+, where standing dead tree data improve disturbance attribution and reduce
 712 uncertainty in greenhouse gas inventories (Mansuy et al., 2024). Together, these dimensions highlight the
 713 feedback between data acquisition, ecological interpretation, predictive modelling, and decision-making, as
 714 summarized in Fig. 4.

715



716

717 **Fig. 4.** Conceptual framework illustrating how standing dead-tree mapping supports ecological analysis and
 718 forest management. a) Multi-source data inputs (e.g., remote sensing imagery, field observations, and manual
 719 annotations) support model training and evaluation for standing dead-tree mapping.
 720 b) Standing dead tree-derived metrics (e.g., affected area, canopy size, mortality stages, and mortality rates)
 721 obtained from high-resolution mapping. c) Ecological interpretation of these metrics, informing forest health
 722 and resilience, including biodiversity, nutrient cycling, and carbon dynamics. d) Applications in forest
 723 management and prediction, including early detection, intervention, wildfire risk assessment, and adaptive
 724 management strategies.

725

726 **6 Current barriers in large-scale standing dead-tree detection**

727 Detecting and mapping standing dead trees at large scales faces multiple ecological, computational, sensor-
728 related, validation, annotation, and operational barriers. In this section, we focus on current barriers, while
729 methodological opportunities and future research priorities are discussed separately in Section 7. Ecologically,
730 forests differ widely in structure, composition, and disturbance regimes, producing standing dead-tree
731 signatures that vary in crown color, foliage loss, and decay dynamics. Boreal conifer stands often exhibit
732 compact crowns with clear discoloration or needle drop, whereas subtropical and tropical broadleaf forests
733 feature multi-layered canopies where standing dead-tree crowns may be obscured by overlapping foliage or
734 persistent understory. Phenology can also shift spectral and textural patterns across seasons. In tropical
735 environments, additional complexities arise because trees may temporarily lose leaves due to seasonal
736 dormancy or stress, and some individuals may resprout after partial defoliation. Standing dead trees can also
737 collapse, fall, be removed, or become obscured by regrowth after initial detection, especially in fast-growing or
738 highly dynamic forests. As a result, single-date observations may misclassify temporarily leafless trees as dead
739 or fail to detect partially dead trees, reducing the temporal validity of mapped standing dead-tree locations.
740 Disturbance processes, including beetle outbreaks, droughts, and windthrow, further shape standing dead-tree
741 trajectories and complicate cross-biome model generalization.

742 Sensor and data limitations further constrain detection. Optical imagery can capture crown discoloration,
743 defoliation, texture, and canopy gaps, but it is sensitive to illumination, shadow, viewing geometry, phenology,
744 and canopy occlusion. Dense or overlapping canopies can obscure partially dead crowns, particularly where
745 mortality occurs below the dominant canopy layer. LiDAR provides valuable structural information, including
746 canopy height, crown geometry, and gap formation, but sparse or ambiguous returns may limit the detection
747 of small, suppressed, or partially occluded standing dead trees. Spatial resolution also creates trade-offs:
748 coarser imagery may obscure individual trees or early mortality symptoms, whereas very high-resolution
749 imagery increases computational demands and may reduce the spatial context available within model input
750 patches. Multi-sensor datasets can help address these limitations, but they also introduce practical challenges,
751 including accurate sub-meter co-registration, compatible acquisition timing, and consistent preprocessing
752 across data sources (Campbell et al., 2020; Marchi et al., 2018).

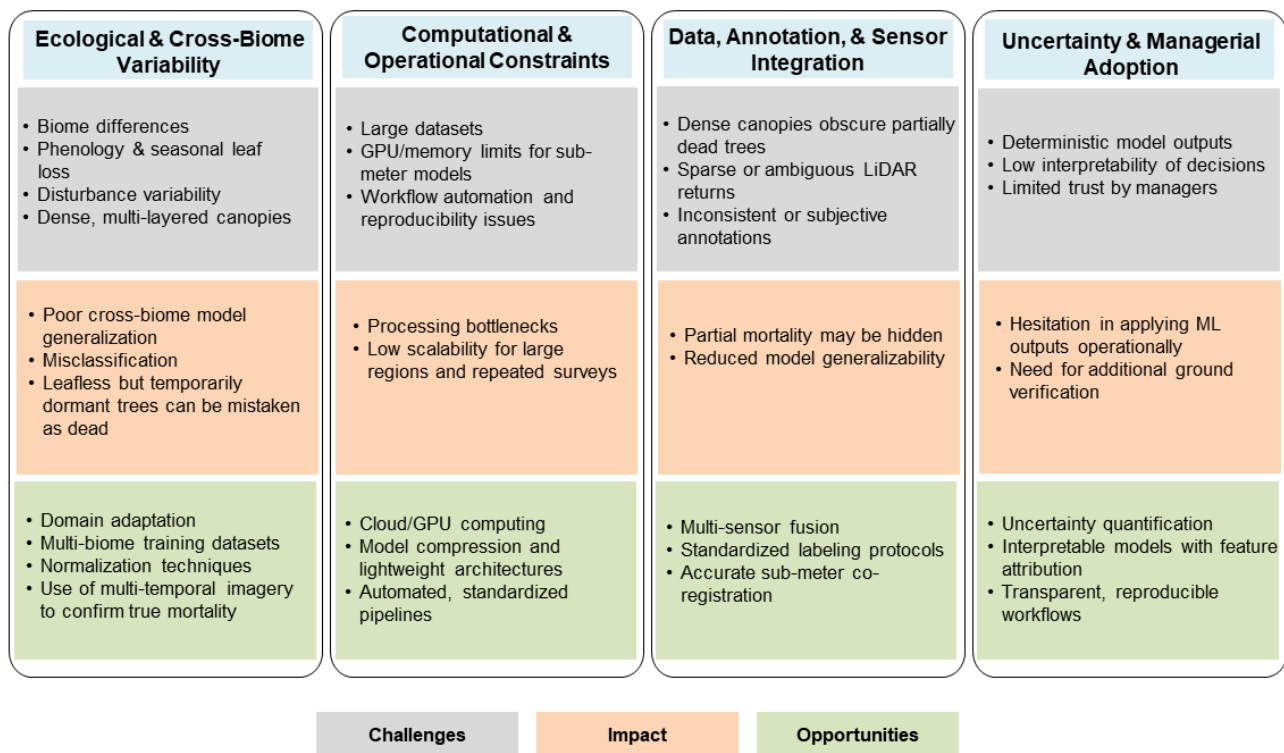
753 Computationally, high-resolution UAV and airborne datasets often reach hundreds of gigabytes or terabyte
754 scale, creating storage, memory, and input/output bottlenecks. Models applied to sub-meter imagery are
755 computationally intensive and often require GPU acceleration, cloud computing, or high-performance
756 computing infrastructure. Large-area inference also requires efficient tiling, mosaicking, post-processing, and
757 quality-control workflows. These requirements can limit reproducibility and operational adoption, especially
758 for forest agencies or conservation organizations with limited computing resources. In addition, complex
759 processing chains involving orthomosaic generation, radiometric normalization, tiling, model inference, post-
760 processing, and map production may be difficult to reproduce unless workflows are clearly documented and
761 standardized.

762 Validation and annotation remain major barriers to model comparability and operational reliability. Most
763 reviewed studies rely primarily on expert image interpretation or withheld image tiles from the same remotely
764 sensed dataset. Although these approaches are useful for evaluating agreement with image-based labels, they

765 do not necessarily confirm whether mapped objects correspond to standing dead trees actually present in the
 766 field. Only a limited number of studies incorporated field observations directly or used mixed field- and image-
 767 based validation. Annotation practices also vary substantially among studies, including pixel masks, crown
 768 polygons, bounding boxes, centroids, patch labels, and canopy mortality fractions. These differences affect both
 769 model training and reported performance, making it difficult to compare results across studies. Inconsistent
 770 definitions of standing dead trees, uncertainty in decay-stage interpretation, omission of partially dead crowns,
 771 and class imbalance further reduce comparability among studies. Therefore, reported performance metrics
 772 often reflect study-specific annotation and validation choices rather than directly comparable model capability.

773 Operational deployment is further constrained by limited model transferability, uncertain reliability, and low
 774 interpretability. Models trained in one region, forest type, biome, or sensor setting may perform poorly
 775 elsewhere because of differences in canopy structure, species composition, illumination, phenology,
 776 disturbance history, and sensor characteristics. Many models also produce deterministic outputs without
 777 uncertainty estimates or interpretable explanations, which can limit trust among forest managers and decision-
 778 makers. This is particularly important when outputs are used for sanitation harvesting, outbreak response,
 779 biodiversity assessment, wildfire-risk planning, or carbon accounting. Large-scale use of UAV, airborne, or very-
 780 high-resolution satellite imagery may also raise concerns related to privacy, land ownership, data access, and
 781 governance. Together, these ecological, sensor-related, computational, validation, annotation, and operational
 782 barriers currently limit the development of scalable and transferable standing dead-tree monitoring systems.
 783 These barriers, their impacts, and the main methodological opportunities for overcoming them are summarized
 784 in Fig. 5.

785



786

787 **Fig. 5.** Conceptual overview of major barriers, impacts, and opportunities in large-scale standing
788 dead-tree detection. Gray boxes summarize current ecological, computational, sensor-related,
789 annotation, and operational challenges. Orange boxes indicate their impacts on model performance,
790 scalability, comparability, and management adoption. Green boxes highlight methodological
791 opportunities discussed in the future research roadmap.

792

793 **7 Discussion and future research roadmap**

794 Future research should move beyond marginal improvements in accuracy metrics alone and focus on
795 developing transferable, interpretable, ecologically meaningful, and operationally scalable standing dead-tree
796 monitoring systems. The most important priorities include standardized benchmark datasets, transferable
797 learning strategies, temporal mortality modelling, multi-sensor fusion, uncertainty quantification,
798 explainability, and responsible data governance.

799 The most urgent need is a large, open, standardized benchmark dataset for standing dead-tree detection and
800 mapping. Such a dataset should include multiple biomes, forest types, disturbance agents, sensor platforms,
801 spatial resolutions, and decay stages. It should also provide clear target definitions, including distinctions
802 among standing dead trees, dead crowns, snags, canopy mortality, fallen deadwood, and declining but not yet
803 dead trees. Standardized annotation protocols are equally important. Future datasets should document
804 whether labels represent crown polygons, bounding boxes, centroids, pixel masks, decay-stage classes, or
805 canopy mortality fractions. Where possible, annotations should be supported by georeferenced field
806 observations, multi-annotator validation, and uncertainty labels. Shared train-test splits and common
807 evaluation metrics would allow more robust comparison among model architectures and reduce the current
808 dependence on study-specific performance claims.

809 Improving model transferability across regions, sensors, and forest types is another central priority. Domain
810 shift remains a major limitation because standing dead-tree appearance varies with biome, species
811 composition, canopy structure, phenology, illumination, and sensor characteristics. Models trained in one
812 landscape may therefore perform poorly when applied to another. Domain adaptation, self-supervised
813 learning, contrastive learning, and few-shot learning offer promising ways to reduce dependence on site-
814 specific annotations and improve cross-site generalization (Kuzu et al., 2024; Yun et al., 2024). These methods
815 can exploit large volumes of unlabeled remote sensing imagery and learn more domain-invariant
816 representations. Future studies should increasingly evaluate models using cross-site, cross-biome, and cross-
817 sensor validation rather than relying only on random splits within the same study area. Such evaluation would
818 provide a more realistic assessment of operational transferability.

819 Standing dead-tree detection should also move beyond simple binary live/dead classification where data allow.
820 Tree mortality is often gradual, progressing through stages of stress, decline, partial dieback, recent death,
821 crown loss, and snag formation. Binary labels can mask ecologically meaningful differences among temporary
822 canopy stress, progressive decline, established mortality, and advanced decay. Multi-temporal remote sensing
823 and deep learning time-series approaches could help distinguish temporary defoliation or seasonal dormancy
824 from true mortality by tracking sequential changes in crown color, canopy density, texture, and structure. These

825 approaches may support earlier detection of tree decline and improve confidence in standing dead-tree
826 classification. Stage-based or confidence-based labels could also improve ecological interpretation by linking
827 detected standing dead trees to decay stage, biodiversity value, and future recruitment of lying deadwood.

828 Future monitoring systems should integrate optical, spectral, structural, and temporal information more
829 effectively. RGB and RGBI imagery provide useful information on crown color and texture, multispectral and
830 hyperspectral data can capture pigment- and moisture-related signals, and LiDAR provides three-dimensional
831 structural information. Combining these data sources can improve detection robustness, especially in dense or
832 heterogeneous forests where no single sensor is sufficient. However, multi-sensor fusion must be supported by
833 scalable processing infrastructure, including automated preprocessing, accurate co-registration, reproducible
834 quality control, cloud-based processing, model compression, and lightweight architectures suitable for large-
835 area inference. UAV-based reference data can also be linked with airborne and satellite observations to support
836 upscaling from local surveys to regional or national standing dead-tree monitoring.

837 Operational monitoring requires more than accurate predictions. Models should provide uncertainty estimates,
838 confidence maps, and interpretable outputs that help users understand where predictions are reliable and
839 where field verification is needed. This is particularly important in complex forests, transitional mortality stages,
840 and regions outside the model's training domain. Explainable AI methods, feature attribution, uncertainty-
841 aware segmentation, and probabilistic outputs can improve trust among forest managers and decision-makers.
842 These outputs could support practical applications such as prioritizing field surveys, detecting disturbance
843 hotspots, planning sanitation harvesting, assessing habitat availability, estimating carbon impacts, and
844 identifying areas of elevated wildfire risk. Future studies should therefore evaluate not only accuracy, but also
845 usefulness for management decisions.

846 Large-scale standing dead-tree monitoring also requires responsible data governance. UAV, airborne, and very-
847 high-resolution satellite imagery may raise concerns related to privacy, land ownership, data access, and
848 equitable participation, especially in landscapes with fragmented ownership or Indigenous and local
849 communities. Transparent communication, inclusive governance, and collaboration with landowners,
850 Indigenous communities, conservation agencies, and forest managers are therefore necessary to ensure that
851 standing dead-tree mapping supports ecological and management goals while respecting local rights and
852 values. Open databases such as deadtrees.earth (Mosig et al., 2026b) and TreeFinder (Wang et al., 2025b)
853 demonstrate the potential of shared, large-scale standing dead-tree resources for benchmarking, collaborative
854 model development, and geographically diverse model training. However, such databases should be well
855 documented, versioned, quality controlled, and maintained over the long term. Clear metadata on sensor type,
856 acquisition date, spatial resolution, annotation protocol, field validation, and uncertainty will be essential for
857 ensuring that these resources remain useful for both research and operational monitoring.

858

859

860

861

862 **Table 3.** Summary of future directions for large-scale standing dead-tree detection and monitoring.

<i>Category</i>	<i>Future research priorities</i>
<i>Technical advances</i>	Self-supervised learning; automated and semi-automated annotation; domain adaptation; multi-sensor fusion; temporal modelling; lightweight edge models; resolution benchmarking; uncertainty quantification; model explainability; standardized benchmarks
<i>Ecological integration</i>	Causes-of-death inference; species-specific responses; mortality trajectories; decay-stage classification; biodiversity-relevant deadwood indicators
<i>Operational deployment</i>	Cloud-based national monitoring systems; early-warning pipelines; UAV-to-satellite model transfer; standardized acquisition and validation protocols; reproducible processing pipelines
<i>Governance and ethics</i>	Privacy safeguards; harmonized legal frameworks; equitable data access; Indigenous and local data governance; transparent data stewardship

863

864 **8 Conclusion**

865 Recent advances in multi-sensor remote sensing and deep learning have substantially improved the detection
 866 and mapping of standing dead trees across a wide range of forest conditions. High-resolution imagery from
 867 uncrewed aerial vehicles, airborne platforms, and satellites, together with LiDAR, multispectral, and
 868 hyperspectral data, now support increasingly detailed assessments of standing dead tree patterns across local
 869 to broader spatial scales. Deep learning approaches, including convolutional neural networks, U-Net
 870 derivatives, object detection frameworks, hybrid models, and more recent transformer-based methods, have
 871 expanded the methodological toolbox available for standing dead-tree detection and mapping. At the same
 872 time, the reviewed studies acknowledge that no single approach is universally optimal, as performance
 873 depends strongly on forest structure, sensor characteristics, annotation quality, and the specific detection or
 874 mapping objective.

875 Despite this progress, large-scale operational monitoring of standing dead trees remains constrained by several
 876 persistent challenges. These include canopy occlusion, class imbalance, inconsistencies in standing dead tree
 877 definitions and annotation protocols, and limited transferability of models across regions, forest types, and
 878 sensor settings. In addition, the ecological complexity of tree mortality, which often develops gradually and
 879 varies among species, disturbance agents, and environments, is not always well captured by simplified live–
 880 dead classification frameworks. As a result, many current approaches remain effective mainly within site-
 881 specific or sensor-specific contexts.

882 Looking forward, operationalizing standing dead-tree mapping at national to global scales will benefit from
 883 integrated pipelines that combine automated preprocessing, multi-sensor data fusion, temporal modeling, and
 884 uncertainty-aware outputs. Embedding ecological knowledge into model design through decay-stage
 885 classification, species-specific spectral signatures, and structural priors can further enhance interpretability and

886 reliability for forest management applications. Open-access, large-scale databases of standing dead trees will
887 accelerate cross-site benchmarking, support label-efficient learning, and facilitate scalable monitoring
888 frameworks.

889 Overall, standing dead-tree mapping is emerging as an important component of forest monitoring, with clear
890 relevance for biodiversity assessment, carbon accounting, disturbance analysis, and early-warning applications.
891 By combining remote sensing, deep learning, and ecological knowledge within transparent and scalable
892 workflows, future research can move the field closer to operational monitoring systems that support forest
893 resilience and climate-adaptation strategies.

894

895 **Acronyms & abbreviations**

896 ADA-Net – Adversarial Domain Adaptation Network
897 AF – Adaptive Filtering
898 ASPP – Atrous Spatial Pyramid Pooling
899 BiFPN – Bidirectional Feature Pyramid Network
900 CCD – Charge-Coupled Device
901 CIR – Color-Infrared
902 CNN – Convolutional Neural Network
903 CO₂ – Carbon Dioxide
904 DMC – Digital Mapping Camera
905 DNN – Deep Neural Network
906 DSFI-YOLO – Dual-Stream Feature Integration YOLO
907 ECA – Efficient Channel Attention
908 IoU – Intersection over Union
909 ES – Edge Smoothing
910 EU – European Union
911 FCN – Fully Convolutional Network
912 FPN – Feature Pyramid Network
913 GAN – Generative Adversarial Network
914 GPU – Graphics Processing Unit
915 I/O – Input / Output
916 IoU – Intersection over Union
917 LDS-YOLO – Lightweight Deep Supervision YOLO
918 LSTM – Long Short-Term Memory
919 MC – Morphological Cleanup
920 MODIS – Moderate Resolution Imaging Spectroradiometer
921 NBR – Normalized Burn Index
922 NDVI – Normalized Difference Vegetation Index
923 RGB – Red, Green, Blue
924 RGBI – Red, Green, Blue, Near-Infrared

925 REDD+ – Reducing Emissions from Deforestation and Forest Degradation
926 ResNet – Residual Network
927 RTK – Real-Time Kinematic
928 SCR – Shape-Constrained Refinement
929 SE – Squeeze-and-Excitation
930 UAV – Uncrewed Aerial Vehicle
931 U-Net – Convolutional Encoder–Decoder Network
932 ViTs – Vision Transformers
933 WIoU – Weighted Intersection over Union
934 WS – Watershed Separation
935 YOLO – You Only Look Once
936

937 **CRedit authorship contribution statement**

938 **Anwarul Islam Chowdhury**: Writing – review & editing, Writing – original draft, Visualization,
939 Investigation, Data curation, Formal analysis, Conceptualization. **Mirela Beloiu**: Writing – review &
940 editing, Writing – original draft, Visualization, Investigation. **Teja Kattenborn**: Writing – review &
941 editing. **Clemens Mosig**: Writing – review & editing. **Mete Ahishali**: Writing – review & editing. **Eetu**
942 **Puttonen**: Writing – review & editing. **Eija Honkavaara**: Writing – review & editing. **Mikko Vastaranta**:
943 Writing – review & editing. **Langning Huo**: Writing – review & editing. **Md. Jamal Uddin**: Writing –
944 review & editing. **Verena C. Griess**: Writing – review & editing. **Anton Kuzmin**: Writing – review &
945 editing. **Yan Cheng**: Visualization, Conceptualization. **Samuli Junntila**: Writing – review & editing,
946 Supervision, Investigation, Conceptualization.

947

948 **Acknowledgement**

949 The authors acknowledge the University of Eastern Finland for open access support. SJ and MA were funded
950 by the European Union (ERC-2023-STG grant agreement no. 101116404). Views and opinions expressed are,
951 however, those of the author(s) only and do not necessarily reflect those of the European Union or the
952 European Research Council Executive Agency. Neither the European Union nor the granting authority can be
953 held responsible for them.

954

955

956

957

958

959

960

961

962 **References**

963

- 964 Aakala, T., Storaunet, K.O., Jonsson, B.G., Korhonen, K.T., 2024. Drivers of snag fall rates in Fennoscandian
965 boreal forests. *Journal of Applied Ecology* 61, 2392–2404. <https://doi.org/10.1111/1365-2664.14729>
- 966 Ahishali, M., Rahman, A.U., Heinaro, E., Junntila, S., 2025. ADA-Net: Attention-Guided Domain Adaptation
967 Network with Contrastive Learning for Standing Dead Tree Segmentation Using Aerial Imagery.
968 <https://doi.org/10.48550/ARXIV.2504.04271>
- 969 Antoniadis, K., Gitas, I.Z., Georgopoulos, N., Stavrakoudis, D., Hadjimitsis, D., 2025. Investigating the potential
970 of ICEYE-SAR data in storm damage detection in a coniferous forest with rugged terrain. *International*
971 *Journal of Remote Sensing* 46, 1622–1651. <https://doi.org/10.1080/01431161.2024.2433761>
- 972 Baldin, C.M., Casella, V.M., 2024. Vegetative Index Intercalibration Between PlanetScope and Sentinel-2
973 Through a SkySat Classification in the Context of “Riserva San Massimo” Rice Farm in Northern Italy.
974 *Remote Sensing* 16, 3921. <https://doi.org/10.3390/rs16213921>
- 975 Bell, D.M., Acker, S.A., Gregory, M.J., Davis, R.J., Garcia, B.A., 2021. Quantifying regional trends in large live
976 tree and snag availability in support of forest management. *Forest Ecology and Management* 479,
977 118554. <https://doi.org/10.1016/j.foreco.2020.118554>
- 978 Beloiu, M., Loeillot, T., Griess, V.C., Poursanidis, D., Petibon, F., 2026. Climate-driven upward spread of forest
979 fires in European mountain regions. *Nat Commun.* <https://doi.org/10.1038/s41467-026-72551-0>
- 980 Bergmüller, K.O., Vanderwel, M.C., 2022. Predicting Tree Mortality Using Spectral Indices Derived from
981 Multispectral UAV Imagery. *Remote Sensing* 14, 2195. <https://doi.org/10.3390/rs14092195>
- 982 Boulton, C.A., Lenton, T.M., Boers, N., 2022. Pronounced loss of Amazon rainforest resilience since the early
983 2000s. *Nat. Clim. Chang.* 12, 271–278. <https://doi.org/10.1038/s41558-022-01287-8>
- 984 Brabcová, V., Tláškal, V., Lepinay, C., Zrůstová, P., Eichlerová, I., Štursová, M., Müller, J., Brandl, R., Bässler, C.,
985 Baldrian, P., 2022. Fungal Community Development in Decomposing Fine Deadwood Is Largely
986 Affected by Microclimate. *Front. Microbiol.* 13, 835274. <https://doi.org/10.3389/fmicb.2022.835274>
- 987 Briechle, S., Krzystek, P., Vosselman, G., 2021. Silvi-Net – A dual-CNN approach for combined classification of
988 tree species and standing dead trees from remote sensing data. *International Journal of Applied Earth*
989 *Observation and Geoinformation* 98, 102292. <https://doi.org/10.1016/j.jag.2020.102292>
- 990 Briechle, S., Krzystek, P., Vosselman, G., 2020. Classification of tree species and standing dead trees by fusing
991 UAV-based lidar data and multispectral imagery in the 3d deep neural network Pointnet++. *ISPRS*
992 *Ann. Photogramm. Remote Sens. Spatial Inf. Sci.* V-2–2020, 203–210. <https://doi.org/10.5194/isprs-annals-V-2-2020-203-2020>
- 994 Brockerhoff, E.G., Barbaro, L., Castagneyrol, B., Forrester, D.I., Gardiner, B., González-Olabarria, J.R., Lyver,
995 P.O., Meurisse, N., Oxbrough, A., Taki, H., Thompson, I.D., Van Der Plas, F., Jactel, H., 2017. Forest
996 biodiversity, ecosystem functioning and the provision of ecosystem services. *Biodivers Conserv* 26,
997 3005–3035. <https://doi.org/10.1007/s10531-017-1453-2>
- 998 Bueno, I.T., Silva, C.A., Anderson-Teixeira, K., Magee, L., Zheng, C., Broadbent, E.N., Zambrano, A.M.A.,
999 Johnson, D.J., 2025. Aboveground Biomass and Tree Mortality Revealed Through Multi-Scale LiDAR
1000 Analysis. *Remote Sensing* 17, 796. <https://doi.org/10.3390/rs17050796>
- 1001 Bujoczek, L., Bujoczek, M., Zięba, S., 2021. Distribution of deadwood and other forest structural indicators
1002 relevant for bird conservation in Natura 2000 special protection areas in Poland. *Sci Rep* 11, 14937.
1003 <https://doi.org/10.1038/s41598-021-94392-1>

- 1004 Campbell, M.J., Dennison, P.E., Tune, J.W., Kannenberg, S.A., Kerr, K.L., Coddling, B.F., Anderegg, W.R.L., 2020.
1005 A multi-sensor, multi-scale approach to mapping tree mortality in woodland ecosystems. *Remote*
1006 *Sensing of Environment* 245, 111853. <https://doi.org/10.1016/j.rse.2020.111853>
- 1007 Catalão, J., Navarro, A., Calvão, J., 2022. Mapping Cork Oak Mortality Using Multitemporal High-Resolution
1008 Satellite Imagery. *Remote Sensing* 14, 2750. <https://doi.org/10.3390/rs14122750>
- 1009 Cheng, Y., Oehmcke, S., Brandt, M., Rosenthal, L., Das, A., Vrieling, A., Saatchi, S., Wagner, F.,
1010 Mugabowindekwe, M., Verbruggen, W., Beier, C., Horion, S., 2024. Scattered tree death contributes
1011 to substantial forest loss in California. *Nat Commun* 15, 641. [https://doi.org/10.1038/s41467-024-](https://doi.org/10.1038/s41467-024-44991-z)
1012 [44991-z](https://doi.org/10.1038/s41467-024-44991-z)
- 1013 Chiang, C.-Y., Barnes, C., Angelov, P., Jiang, R., 2020. Deep Learning-Based Automated Forest Health Diagnosis
1014 From Aerial Images. *IEEE Access* 8, 144064–144076. <https://doi.org/10.1109/ACCESS.2020.3012417>
- 1015 Chowdhury, A.I., Heinaro, E., Tanhuanpää, T., Rahman, A.U., Junttila, S., 2025. Mapping large European aspens
1016 (*Populus tremula* L.) using national aerial imagery and a U-Net convolutional neural network. *Remote*
1017 *Sensing Applications: Society and Environment* 40, 101755.
1018 <https://doi.org/10.1016/j.rsase.2025.101755>
- 1019 Cotrozzi, L., 2022. Spectroscopic detection of forest diseases: a review (1970–2020). *J. For. Res.* 33, 21–38.
1020 <https://doi.org/10.1007/s11676-021-01378-w>
- 1021 Deng, X., Tong, Z., Lan, Y., Huang, Z., 2020. Detection and Location of Dead Trees with Pine Wilt Disease Based
1022 on Deep Learning and UAV Remote Sensing. *AgriEngineering* 2, 294–307.
1023 <https://doi.org/10.3390/agriengineering2020019>
- 1024 Dixon, D.J., Zhu, Y., Brown, C.F., Jin, Y., 2023. Satellite detection of canopy-scale tree mortality and survival
1025 from California wildfires with spatio-temporal deep learning. *Remote Sensing of Environment* 298,
1026 113842. <https://doi.org/10.1016/j.rse.2023.113842>
- 1027 Eliades, F., Sarris, D., Bachofer, F., Michaelides, S., Hadjimitsis, D., 2024. Understanding Tree Mortality
1028 Patterns: A Comprehensive Review of Remote Sensing and Meteorological Ground-Based Studies.
1029 *Forests* 15, 1357. <https://doi.org/10.3390/f15081357>
- 1030 FAO & UNEP, 2020. The State of the World's Forests 2020. FAO and UNEP. <https://doi.org/10.4060/ca8642en>
- 1031 Fassnacht, F.E., White, J.C., Wulder, M.A., Næsset, E., 2024. Remote sensing in forestry: current challenges,
1032 considerations and directions. *Forestry: An International Journal of Forest Research* 97, 11–37.
1033 <https://doi.org/10.1093/forestry/cpad024>
- 1034 Ferrari, L., Waser, L., Psomas, A., Mosig, C., Kattenborn, T., Ginzler, C., Griess, V., Beloiu, M., 2026. Nationwide
1035 deadwood mapping reveals rising mountain forests vulnerability. <https://doi.org/10.31223/X59J3V>
- 1036 Filippelli, S.K., Lefsky, M.A., Rocca, M.E., 2019. Comparison and integration of lidar and photogrammetric
1037 point clouds for mapping pre-fire forest structure. *Remote Sensing of Environment* 224, 154–166.
1038 <https://doi.org/10.1016/j.rse.2019.01.029>
- 1039 Fraver, S., Milo, A.M., Bradford, J.B., D'Amato, A.W., Kenefic, L., Palik, B.J., Woodall, C.W., Brissette, J., 2013.
1040 Woody Debris Volume Depletion Through Decay: Implications for Biomass and Carbon Accounting.
1041 *Ecosystems* 16, 1262–1272. <https://doi.org/10.1007/s10021-013-9682-z>
- 1042 Fricker, G.A., Ventura, J.D., Wolf, J.A., North, M.P., Davis, F.W., Franklin, J., 2019. A Convolutional Neural
1043 Network Classifier Identifies Tree Species in Mixed-Conifer Forest from Hyperspectral Imagery.
1044 *Remote Sensing* 11, 2326. <https://doi.org/10.3390/rs11192326>
- 1045 Ganz, K., Van Wagendonk, L., Khatri-Chhetri, P., Moskal, M., 2025. Spatially explicit forest mortality forecasts
1046 are driven by autocorrelation, not ecological context. <https://doi.org/10.1101/2025.11.19.689366>

- 1047 Gazol, A., Pizarro, M., Hammond, W.M., Allen, C.D., Camarero, J.J., 2025. Droughts preceding tree mortality
1048 events have increased in duration and intensity, especially in dry biomes. *Nat Commun* 16, 5779.
1049 <https://doi.org/10.1038/s41467-025-60856-5>
- 1050 Gevaert, C.M., Aguiar Pedro, A., Ku, O., Cheng, H., Chandramouli, P., Dadrass Javan, F., Nattino, F.,
1051 Georgievska, S., 2025. Explainable few-shot learning workflow for detecting invasive and exotic tree
1052 species. *Sci Rep* 15, 23238. <https://doi.org/10.1038/s41598-025-05394-2>
- 1053 Gonzalez, J.F., Wallner, A., 2025. Robust U-Net Segmentation of Tree Crown Damages in Bavaria, Germany, in:
1054 The 1st International Conference on Advanced Remote Sensing – Shaping Sustainable Global
1055 Landscapes (ICARS 2025). Presented at the ICARS 2025, MDPI, p. 12.
1056 <https://doi.org/10.3390/engproc2025094012>
- 1057 Hall, R.J., Van Der Sanden, J.J., Freeburn, J.T., Thomas, S.J., 2016. Remote sensing of natural disturbance
1058 caused by insect defoliation and dieback: a review (No. 25). <https://doi.org/10.4095/299044>
- 1059 Han, Z., Hu, W., Peng, S., Lin, H., Zhang, J., Zhou, J., Wang, P., Dian, Y., 2022. Detection of Standing Dead Trees
1060 after Pine Wilt Disease Outbreak with Airborne Remote Sensing Imagery by Multi-Scale Spatial
1061 Attention Deep Learning and Gaussian Kernel Approach. *Remote Sensing* 14, 3075.
1062 <https://doi.org/10.3390/rs14133075>
- 1063 Harmon, M.E., Fasth, B.G., Yatskov, M., Kastendick, D., Rock, J., Woodall, C.W., 2020. Release of coarse woody
1064 detritus-related carbon: a synthesis across forest biomes. *Carbon Balance Manage* 15, 1.
1065 <https://doi.org/10.1186/s13021-019-0136-6>
- 1066 Hartmann, H., Bastos, A., Das, A.J., Esquivel-Muelbert, A., Hammond, W.M., Martínez-Vilalta, J., McDowell,
1067 N.G., Powers, J.S., Pugh, T.A.M., Ruthrof, K.X., Allen, C.D., 2022. Climate Change Risks to Global Forest
1068 Health: Emergence of Unexpected Events of Elevated Tree Mortality Worldwide. *Annu. Rev. Plant Biol.*
1069 73, 673–702. <https://doi.org/10.1146/annurev-arplant-102820-012804>
- 1070 Hartmann, H., Battisti, A., Brockerhoff, E.G., Beřka, M., Hurling, R., Jactel, H., Oliva, J., Rouselet, J., Terhonen,
1071 E., Ylioja, T., Melin, M., Olson, Å., De Prins, F., Zhang, K., Åslund, M.S., Davydenko, K., Menkis, A.,
1072 Elfstrand, M., Zúbrik, M., Kunca, A., Galko, J., Paulin, M., Csóka, G., Hoch, G., Pernek, M., Preidl, S.,
1073 Fischer, R., 2025. European forests are under increasing pressure from global change-driven invasions
1074 and accelerating epidemics by insects and diseases. *Journal of Cultivated Plants* 77, 6–24.
1075 <https://doi.org/10.5073/JFK.2025.02.02>
- 1076 Hell, M., Brandmeier, M., Briechle, S., Krzystek, P., 2022. Classification of Tree Species and Standing Dead
1077 Trees with Lidar Point Clouds Using Two Deep Neural Networks: PointCNN and 3DmFV-Net. *PFG* 90,
1078 103–121. <https://doi.org/10.1007/s41064-022-00200-4>
- 1079 Hemming-Schroeder, N.M., Gutierrez, A.A., Allison, S.D., Randerson, J.T., 2023. Estimating Individual Tree
1080 Mortality in the Sierra Nevada Using Lidar and Multispectral Reflectance Data. *JGR Biogeosciences*
1081 128, e2022JG007234. <https://doi.org/10.1029/2022JG007234>
- 1082 Hlásny, T., Zimová, S., Bentz, B., 2021. Scientific response to intensifying bark beetle outbreaks in Europe and
1083 North America. *Forest Ecology and Management* 499, 119599.
1084 <https://doi.org/10.1016/j.foreco.2021.119599>
- 1085 International Tree Mortality Network, 2025. Towards a global understanding of tree mortality. *New*
1086 *Phytologist* 245, 2377–2392. <https://doi.org/10.1111/nph.20407>
- 1087 Jääskeläinen, J.J., 2024. Mapping forest canopy mortality area using PlanetScope satellite imagery and deep
1088 learning. Master’s thesis, University of Helsinki. <http://hdl.handle.net/10138/589513>
- 1089 Jiang, S., Yao, W., Heurich, M., 2019. Dead wood detection based on semantic segmentation of vhr aerial cir
1090 imagery using optimized fcn-densenet. *Int. Arch. Photogramm. Remote Sens. Spatial Inf. Sci.* XLII-
1091 2/W16, 127–133. <https://doi.org/10.5194/isprs-archives-XLII-2-W16-127-2019>

- 1092 Jiang, X., Wu, Z., Han, S., Yan, H., Zhou, B., Li, J., 2023. A multi-scale approach to detecting standing dead trees
1093 in UAV RGB images based on improved faster R-CNN. *PLoS ONE* 18, e0281084.
1094 <https://doi.org/10.1371/journal.pone.0281084>
- 1095 Jin, Y., Xu, M., Zheng, J., 2023. Automatic Detection of Dead Trees Based on Lightweight YOLOv4 and UAV
1096 Imagery. *JIPS(Journal of Information Processing Systems)* 19, 614–630.
1097 <https://doi.org/10.3745/JIPS.02.0204>
- 1098 Joshi, D., Witharana, C., 2025. Vision Transformer-Based Unhealthy Tree Crown Detection in Mixed
1099 Northeastern US Forests and Evaluation of Annotation Uncertainty. *Remote Sensing* 17, 1066.
1100 <https://doi.org/10.3390/rs17061066>
- 1101 Junttila, S., 2025. Remote sensing approaches for assessing and monitoring forest health, in: *Forest*
1102 *Microbiology*. Elsevier, pp. 419–431. <https://doi.org/10.1016/B978-0-443-21903-0.00025-4>
- 1103 Junttila, S., Blomqvist, M., Laukkanen, V., Heinaro, E., Polvivaara, A., O’Sullivan, H., Yrttimaa, T., Vastaranta, M.,
1104 Peltola, H., 2024. Significant increase in forest canopy mortality in boreal forests in Southeast Finland.
1105 *Forest Ecology and Management* 565, 122020. <https://doi.org/10.1016/j.foreco.2024.122020>
- 1106 Jutras-Perreault, M.-C., Næsset, E., Gobakken, T., Ørka, H.O., 2023. Detecting the presence of standing dead
1107 trees using airborne laser scanning and optical data. *Scandinavian Journal of Forest Research* 38, 208–
1108 220. <https://doi.org/10.1080/02827581.2023.2211807>
- 1109 Kattenborn, T., Leitloff, J., Schiefer, F., Hinz, S., 2021. Review on Convolutional Neural Networks (CNN) in
1110 vegetation remote sensing. *ISPRS Journal of Photogrammetry and Remote Sensing* 173, 24–49.
1111 <https://doi.org/10.1016/j.isprsjprs.2020.12.010>
- 1112 Khatri-Chhetri, P., Van Wagendonk, L., Hendryx, S.M., Kane, V.R., 2024. Enhancing individual tree mortality
1113 mapping: The impact of models, data modalities, and classification taxonomy. *Remote Sensing of*
1114 *Environment* 300, 113914. <https://doi.org/10.1016/j.rse.2023.113914>
- 1115 Korpela, I., Polvivaara, A., Papunen, S., Tienaho, N., Jaakkola, L., Uotila, J., Puputti, T., Flyktman, A., 2023.
1116 Airborne dual-wavelength waveform LiDAR improves species classification accuracy of boreal
1117 broadleaved and coniferous trees. *Silva Fenn* 56. <https://doi.org/10.14214/sf.22007>
- 1118 Krizhevsky, A., Sutskever, I., Hinton, G.E., 2012. ImageNet Classification with Deep Convolutional Neural
1119 Networks, in: Pereira, F., Burges, C.J., Bottou, L., Weinberger, K.Q. (Eds.), *Advances in Neural*
1120 *Information Processing Systems*. Curran Associates, Inc.
- 1121 Krzystek, P., Serebryanyk, A., Schnörr, C., Červenka, J., Heurich, M., 2020. Large-Scale Mapping of Tree Species
1122 and Dead Trees in Šumava National Park and Bavarian Forest National Park Using Lidar and
1123 Multispectral Imagery. *Remote Sensing* 12, 661. <https://doi.org/10.3390/rs12040661>
- 1124 Kuzmin, A., Korhonen, L., Tanhuanpää, T., Kukkonen, M., Maltamo, M., Kumpula, T., 2026. Classification of
1125 tree species and standing dead trees in Boreal forests using UAV-based RGB, multispectral, and LiDAR
1126 point clouds. *Remote Sens Ecol Conserv* rse2.70070. <https://doi.org/10.1002/rse2.70070>
- 1127 Kuzu, R.S., Antropov, O., Molinier, M., Dumitru, C.O., Saha, S., Zhu, X.X., 2024. Forest Disturbance Detection
1128 via Self-Supervised and Transfer Learning With Sentinel-1&2 Images. *IEEE J. Sel. Top. Appl. Earth*
1129 *Observations Remote Sensing* 17, 4751–4767. <https://doi.org/10.1109/JSTARS.2024.3361183>
- 1130 Leidemer, T., Lopez Caceres, M.L., Diez, Y., Ferracini, C., Tsou, C.-Y., Katahira, M., 2025. Evaluation of Temporal
1131 Trends in Forest Health Status Using Precise Remote Sensing. *Drones* 9, 337.
1132 <https://doi.org/10.3390/drones9050337>
- 1133 Lines, E.R., Allen, M., Cabo, C., Calders, K., Debus, A., Grieve, S.W.D., Miltiadou, M., Noach, A., Owen, H.J.F.,
1134 Puliti, S., 2022. AI applications in forest monitoring need remote sensing benchmark datasets, in:
1135 2022 IEEE International Conference on Big Data (Big Data). Presented at the 2022 IEEE International

- 1136 Conference on Big Data (Big Data), IEEE, Osaka, Japan, pp. 4528–4533.
1137 <https://doi.org/10.1109/BigData55660.2022.10020772>
- 1138 Liu, Q., Peng, C., Schneider, R., Cyr, D., McDowell, N.G., Kneeshaw, D., 2023. Drought-induced increase in tree
1139 mortality and corresponding decrease in the carbon sink capacity of Canada’s boreal forests from
1140 1970 to 2020. *Global Change Biology* 29, 2274–2285. <https://doi.org/10.1111/gcb.16599>
- 1141 Liu, X., Frey, J., Denter, M., Zielewska-Büttner, K., Still, N., Koch, B., 2021. Mapping standing dead trees in
1142 temperate montane forests using a pixel- and object-based image fusion method and stereo
1143 WorldView-3 imagery. *Ecological Indicators* 133, 108438.
1144 <https://doi.org/10.1016/j.ecolind.2021.108438>
- 1145 Löfroth, T., Birkemoe, T., Shorohova, E., Dynesius, M., Fenton, N.J., Drapeau, P., Tremblay, J.A., 2023.
1146 Deadwood Biodiversity, in: Girona, M.M., Morin, H., Gauthier, S., Bergeron, Y. (Eds.), *Boreal Forests in
1147 the Face of Climate Change, Advances in Global Change Research*. Springer International Publishing,
1148 Cham, pp. 167–189. https://doi.org/10.1007/978-3-031-15988-6_6
- 1149 Long, J., Shelhamer, E., Darrell, T., 2014. Fully Convolutional Networks for Semantic Segmentation.
1150 <https://doi.org/10.48550/ARXIV.1411.4038>
- 1151 Losso, A., Challis, A., Gauthey, A., Nolan, R.H., Hislop, S., Roff, A., Boer, M.M., Jiang, M., Medlyn, B.E., Choat,
1152 B., 2022. Canopy dieback and recovery in Australian native forests following extreme drought. *Sci Rep*
1153 12, 21608. <https://doi.org/10.1038/s41598-022-24833-y>
- 1154 Lucas, M., Pukrop, M., Beckschäfer, P., Waske, B., 2024. Individual tree detection and crown delineation in the
1155 Harz National Park from 2009 to 2022 using mask R–CNN and aerial imagery. *ISPRS Open Journal of
1156 Photogrammetry and Remote Sensing* 13, 100071. <https://doi.org/10.1016/j.ophoto.2024.100071>
- 1157 Luo, Y., Wei, N., Lu, X., Zhou, Y., Tao, F., Quan, Q., Liao, C., Jiang, L., Xia, J., Huang, Y., Niu, S., Xu, X., Sun, Y.,
1158 Zeng, N., Koven, C., Peng, L., Davis, S., Smith, P., You, F., Jiang, Y., Cheng, L., Houlton, B., 2025. Large
1159 CO2 removal potential of woody debris preservation in managed forests. *Nat. Geosci.* 18, 675–681.
1160 <https://doi.org/10.1038/s41561-025-01731-2>
- 1161 Lv, H., Wang, G., Chen, W., Zou, T., Zhou, Y., Shi, Y., 2025. Impacts of stand structure characteristics of three
1162 forest types on the internal environment and carbon sink functions of forests. *Ecological Indicators*
1163 179, 114199. <https://doi.org/10.1016/j.ecolind.2025.114199>
- 1164 Ma, Y., Chen, S., Ermon, S., Lobell, D.B., 2024. Transfer learning in environmental remote sensing. *Remote
1165 Sensing of Environment* 301, 113924. <https://doi.org/10.1016/j.rse.2023.113924>
- 1166 Mahanta, D.K., Bhoi, T.K., Komal, J., Samal, I., Mastinu, A., 2024. Spatial, spectral and temporal insights:
1167 harnessing high-resolution satellite remote sensing and artificial intelligence for early monitoring of
1168 wood boring pests in forests. *Plant Stress* 11, 100381. <https://doi.org/10.1016/j.stress.2024.100381>
- 1169 Manfreda, S., McCabe, M.F., Miller, P.E., Lucas, R., Pajuelo Madrigal, V., Mallinis, G., Ben Dor, E., Helman, D.,
1170 Estes, L., Ciraolo, G., Müllerová, J., Tauro, F., De Lima, M.I., De Lima, J.L.M.P., Maltese, A., Frances, F.,
1171 Caylor, K., Kohv, M., Perks, M., Ruiz-Pérez, G., Su, Z., Vico, G., Toth, B., 2018. On the Use of Unmanned
1172 Aerial Systems for Environmental Monitoring. *Remote Sensing* 10, 641.
1173 <https://doi.org/10.3390/rs10040641>
- 1174 Mansuy, N., Barredo, J.I., Migliavacca, M., Pilli, R., Leverkus, A.B., Janouskova, K., Mubareka, S., 2024.
1175 Reconciling the different uses and values of deadwood in the European Green Deal. *One Earth* 7,
1176 1542–1558. <https://doi.org/10.1016/j.oneear.2024.08.001>
- 1177 Marchi, N., Pirotti, F., Lingua, E., 2018. Airborne and Terrestrial Laser Scanning Data for the Assessment of
1178 Standing and Lying Deadwood: Current Situation and New Perspectives. *Remote Sensing* 10, 1356.
1179 <https://doi.org/10.3390/rs10091356>

- 1180 Martinuzzi, S., Vierling, L.A., Gould, W.A., Falkowski, M.J., Evans, J.S., Hudak, A.T., Vierling, K.T., 2009. Mapping
1181 snags and understory shrubs for a LiDAR-based assessment of wildlife habitat suitability. *Remote*
1182 *Sensing of Environment* 113, 2533–2546. <https://doi.org/10.1016/j.rse.2009.07.002>
- 1183 Matejčíková, J., Věbrová, D., Surový, P., 2024. Comparative Analysis of Machine Learning Techniques and Data
1184 Sources for Dead Tree Detection: What Is the Best Way to Go? *Remote Sensing* 16, 3086.
1185 <https://doi.org/10.3390/rs16163086>
- 1186 Mäyrä, J., Tanhuanpää, T., Kuzmin, A., Heinaro, E., Kumpula, T., Vihervaara, P., 2025. Using UAV images and
1187 deep learning to enhance the mapping of deadwood in boreal forests. *Remote Sensing of*
1188 *Environment* 329, 114906. <https://doi.org/10.1016/j.rse.2025.114906>
- 1189 McNicol, I.M., Mitchard, E.T.A., Aquino, C., Burt, A., Carstairs, H., Dassi, C., Modinga Dikongo, A., Disney, M.I.,
1190 2021. To What Extent Can UAV Photogrammetry Replicate UAV LiDAR to Determine Forest Structure?
1191 A Test in Two Contrasting Tropical Forests. *JGR Biogeosciences* 126, e2021JG006586.
1192 <https://doi.org/10.1029/2021JG006586>
- 1193 Merganičová, K., Merganič, J., Svoboda, M., Bače, R., Šebeň, V., 2012. Deadwood in Forest Ecosystems, in:
1194 *Forest Ecosystems-More than Just Trees*. IntechOpen. doi: 10.5772/31003
- 1195 Miltiadou, M., Agapiou, A., Gonzalez Aracil, S., Hadjimitsis, D.G., 2020. Detecting Dead Standing Eucalypt
1196 Trees from Voxellised Full-Waveform Lidar Using Multi-Scale 3D-Windows for Tackling Height and Size
1197 Variations. *Forests* 11, 161. <https://doi.org/10.3390/f11020161>
- 1198 Miltiadou, M., Campbell, N.D.F., Gonzalez Aracil, S., Brown, T., Grant, M.G., 2018. Detection of dead standing
1199 *Eucalyptus camaldulensis* without tree delineation for managing biodiversity in native Australian
1200 forest. *International Journal of Applied Earth Observation and Geoinformation* 67, 135–147.
1201 <https://doi.org/10.1016/j.jag.2018.01.008>
- 1202 Möhring, J., Kattenborn, T., Mahecha, M.D., Cheng, Y., Beloiu Schwenke, M., Cloutier, M., Denter, M., Frey, J.,
1203 Gassilloud, M., Göritz, A., Hempel, J., Horion, S., Jucker, T., Junttila, S., Khatri-Chhetri, P., Korznikov, K.,
1204 Kruse, S., Laliberté, E., Maroschek, M., Neumeier, P., Pérez-Priego, O., Potts, A., Schiefer, F., Seidl, R.,
1205 Vajna-Jehle, J., Zielewska-Büttner, K., Mosig, C., 2025. Global, multi-scale standing deadwood
1206 segmentation in centimeter-scale aerial images. *ISPRS Open Journal of Photogrammetry and Remote*
1207 *Sensing* 18, 100104. <https://doi.org/10.1016/j.ophoto.2025.100104>
- 1208 Mori, A.S., Lertzman, K.P., Gustafsson, L., 2017. Biodiversity and ecosystem services in forest ecosystems: a
1209 research agenda for applied forest ecology. *Journal of Applied Ecology* 54, 12–27.
1210 <https://doi.org/10.1111/1365-2664.12669>
- 1211 Mosig, C., Kattenborn, T., Montero Loaiza, D., Vanja-Jehle, J., Brandt, J., Jacobs, N., Khanal, S., Xing, E.,
1212 Schwartz, M., Muller-Landau, H.C., Beloiu, M., Bozzini, A., Cheng, Y., Ganz, K., Grüning, B., Hartmann,
1213 H., Hempel, J., Horion, S., Junttila, S., Korznikov, K., Kraemer, G., Mönks, M., Nardi, D., Neumeier, P.,
1214 Schmid, J., Soltani, S., Therese-Schmehl, M., Veitch-Michaelis, J., Mahecha, M., 2026a. Sub-pixel
1215 mapping of disturbance and tree mortality dynamics from Sentinel-2 time series around the globe.
1216 <https://doi.org/10.31223/X5B18W>
- 1217 Mosig, C., Vajna-Jehle, J., Mahecha, M.D., Cheng, Y., Hartmann, H., Montero, D., Junttila, S., Horion, S.,
1218 Schwenke, M.B., Koontz, M.J., Maulud, K.N.A., Adu-Bredu, S., Al-Halbouni, D., Ali, M., Allen, M.,
1219 Altman, J., Amorós, L., Angiolini, C., Astrup, R., Awada, H., Barrasso, C., Bartholomeus, H., Beck, P.S.A.,
1220 Bozzini, A., Braun-Wimmer, J., Brede, B., Breunig, F.M., Brugnaro, S., Buras, A., Burchard-Levine, V.,
1221 Camarero, J.J., Candotti, A., Capuder, L., Carrieri, E., Centritto, M., Chirici, G., Cloutier, M., Conciani, D.,
1222 Cushman, K., Dalling, J.W., Dao, P.D., Dempewolf, J., Denter, M., Dogotari, M., Díaz-Delgado, R., Ecke,
1223 S., Eichel, J., Eltner, A., Fabbri, A., Fabi, M., Fassnacht, F., Ferreira, M.P., Fischer, F.J., Frey, J., Frick, A.,
1224 Fuentes, J., Ganz, S., Garbarino, M., García, M., Gassilloud, M., Gazol, A., Gea-Izquierdo, G.,

- 1225 Gerberding, K., Ghasemi, M., Giannetti, F., Gillan, J., Gonzalez, R., Gosper, C., Greene, T., Greinwald,
1226 K., Grieve, S., Große-Stoltenberg, A., Gutierrez, J.A., Göritz, A., Hajek, P., Hedding, D., Hempel, J.,
1227 Heremans, S., Hernández, M., Heurich, M., Honkavaara, E., Höfle, B., Jackisch, R., Jucker, T., Kalwij,
1228 J.M., Kepfer-Rojas, S., Khatri-Chhetri, P., Kleinebecker, T., Klemmt, H.-J., Klouček, T., Koivumäki, N.,
1229 Kolagani, N., Komárek, J., Korznikov, K., Kraszewski, B., Kruse, S., Krüger, R., Kuechly, H., Kwong, I.H.Y.,
1230 Laliberté, E., Langan, L., Latifi, H., Leal-Medina, C., Lehmann, J.R.K., Li, L., Lines, E., Lisiewicz, M.,
1231 Lopatin, J., Lucieer, A., Ludwig, A., Ludwig, M., Lyytikäinen-Saarenmaa, P., Ma, Q., Mansuy, N., Peña,
1232 J.M., Marino, G., Maroschek, M., Martín, M.P., Martín-Benito, D., Matham, P., Mazzoni, S., Meloni, F.,
1233 Menzel, A., Meyer, H., Miraki, M., Moreno, G., Moreno-Fernández, D., Muller-Landau, H.C., Mälikke,
1234 M., Möhring, J., Müllerova, J., Naidu, S.S., Nardi, D., Neumeier, P., Nita, M.D., Näsi, R., Oppgenoorh,
1235 L., Orunbaev, S., Palmer, M., Paul, T., Pfenning, M., Potts, A., Prasanna, G.L., Prober, S., Puliti, S., Pérez-
1236 Luque, A.J., Pérez-Priego, O., Reudenbach, C., Revuelto, J., Rivas-Torres, G., Roberge, P., Roggero, P.P.,
1237 Rossi, C., Ruehr, N.K., Ruiz-Benito, P., Runge, C.M., Satta, G.G.A., Scanu, B., Scherer-Lorenzen, M.,
1238 Schiefer, F., Schiller, C., Schladebach, J., Schmehl, M.-T., Schmid, J., Schmidt, T.A., Schwarz, S., Seidl, R.,
1239 Seifert, T., Barba, A.S., Shafeian, E., Shapiro, A., De Simone, L., Sohrabi, H., Soltani, S., Sotomayor, L.,
1240 Sparrow, B., Steer, B.S.C., Stenson, M., Stöckigt, B., Su, Y., Suomalainen, J., Tamudo, E., Barbieri, M.J.T.,
1241 Tomelleri, E., Torresani, M., Trepekli, K., Ullah, Saif, Ullah, Sami, Umlauf, J., Vargas-Ramírez, N.,
1242 Vatandaslar, C., Visacki, V., Volpi, M., Vásquez, V., Wallis, C., Weinstein, B., Weiser, H., Wich, S.,
1243 Ximena, T.C., Zarco-Tejada, P.J., Zdunic, K., Zielewska-Büttner, K., De Oliveira, R.A., Van Wagendonk,
1244 L., Von Dösky, V., Kattenborn, T., 2026b. deadtrees.earth — An open-access and interactive database
1245 for centimeter-scale aerial imagery to uncover global tree mortality dynamics. *Remote Sensing of*
1246 *Environment* 332, 115027. <https://doi.org/10.1016/j.rse.2025.115027>
- 1247 Ni, M., Wu, Q., Li, G., Li, D., 2025. Remote Sensing Technology for Observing Tree Mortality and Its Influences
1248 on Carbon–Water Dynamics. *Forests* 16, 194. <https://doi.org/10.3390/f16020194>
- 1249 Oberle, B., Ogle, K., Zanne, A.E., Woodall, C.W., 2018. When a tree falls: Controls on wood decay predict
1250 standing dead tree fall and new risks in changing forests. *PLoS ONE* 13, e0196712.
1251 <https://doi.org/10.1371/journal.pone.0196712>
- 1252 Pan, Y., Birdsey, R.A., Fang, J., Houghton, R., Kauppi, P.E., Kurz, W.A., Phillips, O.L., Shvidenko, A., Lewis, S.L.,
1253 Canadell, J.G., Ciais, P., Jackson, R.B., Pacala, S.W., McGuire, A.D., Piao, S., Rautiainen, A., Sitch, S.,
1254 Hayes, D., 2011. A Large and Persistent Carbon Sink in the World’s Forests. *Science* 333, 988–993.
1255 <https://doi.org/10.1126/science.1201609>
- 1256 Piaszczyk, W., Lasota, J., Błońska, E., 2019. Effect of Organic Matter Released from Deadwood at Different
1257 Decomposition Stages on Physical Properties of Forest Soil. *Forests* 11, 24.
1258 <https://doi.org/10.3390/f11010024>
- 1259 Polewski, P., Shelton, J., Yao, W., Heurich, M., 2020. Segmentation of single standing dead trees in high-
1260 resolution aerial imagery with generative adversarial network-based shape priors. *Int. Arch.*
1261 *Photogramm. Remote Sens. Spatial Inf. Sci.* XLIII-B2-2020, 717–723. [https://doi.org/10.5194/isprs-
1262 archives-XLIII-B2-2020-717-2020](https://doi.org/10.5194/isprs-archives-XLIII-B2-2020-717-2020)
- 1263 Polewski, P., Yao, W., Heurich, M., Krzystek, P., Stilla, U., 2015a. Detection of single standing dead trees from
1264 aerial color infrared imagery by segmentation with shape and intensity priors. *ISPRS Ann.*
1265 *Photogramm. Remote Sens. Spatial Inf. Sci.* II-3/W4, 181–188. [https://doi.org/10.5194/isprsannals-II-
1266 3-W4-181-2015](https://doi.org/10.5194/isprsannals-II-3-W4-181-2015)
- 1267 Polewski, P., Yao, W., Heurich, M., Krzystek, P., Stilla, U., 2015b. Active learning approach to detecting standing
1268 dead trees from ALS point clouds combined with aerial infrared imagery, in: 2015 IEEE Conference on
1269 Computer Vision and Pattern Recognition Workshops (CVPRW). Presented at the 2015 IEEE

- 1270 Conference on Computer Vision and Pattern Recognition Workshops (CVPRW), IEEE, Boston, MA,
1271 USA, pp. 10–18. <https://doi.org/10.1109/CVPRW.2015.7301378>
- 1272 Polvivaara, A., Korpela, I., Vastaranta, M., Junttila, S., 2024. Detecting tree mortality using waveform features
1273 of airborne LiDAR. *Remote Sensing of Environment* 303, 114019.
1274 <https://doi.org/10.1016/j.rse.2024.114019>
- 1275 Rahman, A.U., Heinaro, E., Ahishali, M., Junttila, S., 2025. Dual-task learning for dead tree detection and
1276 segmentation with hybrid self-attention U-Nets in aerial imagery. *International Journal of Applied*
1277 *Earth Observation and Geoinformation* 144, 104851. <https://doi.org/10.1016/j.jag.2025.104851>
- 1278 Rondeux, J., Sanchez, C., 2010. Review of indicators and field methods for monitoring biodiversity within
1279 national forest inventories. Core variable: Deadwood. *Environ Monit Assess* 164, 617–630.
1280 <https://doi.org/10.1007/s10661-009-0917-6>
- 1281 Ronneberger, O., Fischer, P., Brox, T., 2015. U-Net: Convolutional Networks for Biomedical Image
1282 Segmentation. <https://doi.org/10.48550/ARXIV.1505.04597>
- 1283 Sani-Mohammed, A., Yao, W., Heurich, M., 2022. Instance segmentation of standing dead trees in dense
1284 forest from aerial imagery using deep learning. *ISPRS Open Journal of Photogrammetry and Remote*
1285 *Sensing* 6, 100024. <https://doi.org/10.1016/j.ophoto.2022.100024>
- 1286 Schelhaas, M., Nabuurs, G., Schuck, A., 2003. Natural disturbances in the European forests in the 19th and
1287 20th centuries. *Global Change Biology* 9, 1620–1633. <https://doi.org/10.1046/j.1365-2486.2003.00684.x>
- 1289 Schiefer, F., Kattenborn, T., Frick, A., Frey, J., Schall, P., Koch, B., Schmidlein, S., 2020. Mapping forest tree
1290 species in high resolution UAV-based RGB-imagery by means of convolutional neural networks. *ISPRS*
1291 *Journal of Photogrammetry and Remote Sensing* 170, 205–215.
1292 <https://doi.org/10.1016/j.isprsjprs.2020.10.015>
- 1293 Schiefer, F., Schmidlein, S., Frick, A., Frey, J., Klinke, R., Zielewska-Büttner, K., Junttila, S., Uhl, A., Kattenborn,
1294 T., 2023. UAV-based reference data for the prediction of fractional cover of standing deadwood from
1295 Sentinel time series. *ISPRS Open Journal of Photogrammetry and Remote Sensing* 8, 100034.
1296 <https://doi.org/10.1016/j.ophoto.2023.100034>
- 1297 Schiefer, F., Schmidlein, S., Hartmann, H., Schnabel, F., Kattenborn, T., 2025. Large-scale remote sensing
1298 reveals that tree mortality in Germany appears to be greater than previously expected. *Forestry: An*
1299 *International Journal of Forest Research* 98, 535–549. <https://doi.org/10.1093/forestry/cpae062>
- 1300 Schiller, C., Költzow, J., Schwarz, S., Schiefer, F., Fassnacht, F.E., 2024. Forest disturbance detection in Central
1301 Europe using transformers and Sentinel-2 time series. *Remote Sensing of Environment* 315, 114475.
1302 <https://doi.org/10.1016/j.rse.2024.114475>
- 1303 Schwarz, S., Werner, C., Fassnacht, F.E., Ruehr, N.K., 2024. Forest canopy mortality during the 2018-2020
1304 summer drought years in Central Europe: The application of a deep learning approach on aerial
1305 images across Luxembourg. *Forestry: An International Journal of Forest Research* 97, 376–387.
1306 <https://doi.org/10.1093/forestry/cpad049>
- 1307 Schwenke, M.B., Berger, E., Ecke, S., Xia, Z., Reichmuth, C., Gessler, A., Klemmt, H.-J., Glatthorn, J., Stillhard, J.,
1308 Griess, V., Waser, L.T., 2025. Tree Crown Mortality and Defoliation Assessment in Temperate Forests
1309 Using Aerial Imagery and Deep Learning. <https://doi.org/10.2139/ssrn.5360617>
- 1310 Seibold, S., Thorn, S., 2018. The Importance of Dead-Wood Amount for Saproxyllic Insects and How It Interacts
1311 with Dead-Wood Diversity and Other Habitat Factors, in: Ulyshen, M.D. (Ed.), *Saproxyllic Insects*,
1312 *Zoological Monographs*. Springer International Publishing, Cham, pp. 607–637.
1313 https://doi.org/10.1007/978-3-319-75937-1_18

- 1314 Seidl, R., Thom, D., Kautz, M., Martin-Benito, D., Peltoniemi, M., Vacchiano, G., Wild, J., Ascoli, D., Petr, M.,
1315 Honkaniemi, J., Lexer, M.J., Trotsiuk, V., Mairota, P., Svoboda, M., Fabrika, M., Nagel, T.A., Reyer,
1316 C.P.O., 2017. Forest disturbances under climate change. *Nature Clim Change* 7, 395–402.
1317 <https://doi.org/10.1038/nclimate3303>
- 1318 Seidling, W., Travaglini, D., Meyer, P., Waldner, P., Fischer, R., Granke, O., Chirici, G., Corona, P., 2014. Dead
1319 wood and stand structure - relationships for forest plots across Europe. *iForest* 7, 269–281.
1320 <https://doi.org/10.3832/ifor1057-007>
- 1321 Senf, C., Seidl, R., 2021. Mapping the forest disturbance regimes of Europe. *Nat Sustain* 4, 63–70.
1322 <https://doi.org/10.1038/s41893-020-00609-y>
- 1323 Shahinfar, S., Meek, P., Falzon, G., 2020. “How many images do I need?” Understanding how sample size per
1324 class affects deep learning model performance metrics for balanced designs in autonomous wildlife
1325 monitoring. *Ecological Informatics* 57, 101085. <https://doi.org/10.1016/j.ecoinf.2020.101085>
- 1326 Shannon, V.L., Vanguelova, E.I., Morison, J.I.L., Shaw, L.J., Clark, J.M., 2022. The contribution of deadwood to
1327 soil carbon dynamics in contrasting temperate forest ecosystems. *Eur J Forest Res* 141, 241–252.
1328 <https://doi.org/10.1007/s10342-021-01435-3>
- 1329 Shelton, J.A., Polewski, P., Yao, W., Heurich, M., 2021. A hybrid convolutional neural network/active contour
1330 approach to segmenting dead trees in aerial imagery. <https://doi.org/10.48550/ARXIV.2112.02725>
- 1331 Sheykhmousa, M., Mahdianpari, M., Ghanbari, H., Mohammadimanesh, F., Ghamisi, P., Homayouni, S., 2020.
1332 Support Vector Machine Versus Random Forest for Remote Sensing Image Classification: A Meta-
1333 Analysis and Systematic Review. *IEEE J. Sel. Top. Appl. Earth Observations Remote Sensing* 13, 6308–
1334 6325. <https://doi.org/10.1109/JSTARS.2020.3026724>
- 1335 Shields, S.G., Coops, N.C., Achim, A., Hamelin, R.C., Mulverhill, C., 2025. A review of PlanetScope CubeSats for
1336 forest monitoring. *Science of Remote Sensing* 12, 100314. <https://doi.org/10.1016/j.srs.2025.100314>
- 1337 Steier, J., Goebel, M., Iwaszczuk, D., 2024. Is Your Training Data Really Ground Truth? A Quality Assessment of
1338 Manual Annotation for Individual Tree Crown Delineation. *Remote Sensing* 16, 2786.
1339 <https://doi.org/10.3390/rs16152786>
- 1340 Steinebrunner, F., Tischer, A., Medicus, T., Huth, F., Bernhardt-Römermann, M., 2025. The effects of
1341 deadwood on tree regeneration and microsites: A systematic review. *Forest Ecology and*
1342 *Management* 596, 123096. <https://doi.org/10.1016/j.foreco.2025.123096>
- 1343 Sylvain, J.-D., Drolet, G., Brown, N., 2019. Mapping dead forest cover using a deep convolutional neural
1344 network and digital aerial photography. *ISPRS Journal of Photogrammetry and Remote Sensing* 156,
1345 14–26. <https://doi.org/10.1016/j.isprsjprs.2019.07.010>
- 1346 Tao, H., Li, C., Zhao, D., Deng, S., Hu, H., Xu, X., Jing, W., 2020. Deep learning-based dead pine tree detection
1347 from unmanned aerial vehicle images. *International Journal of Remote Sensing* 41, 8238–8255.
1348 <https://doi.org/10.1080/01431161.2020.1766145>
- 1349 Turkulainen, E., Honkavaara, E., Näsi, R., Oliveira, R.A., Hakala, T., Junntila, S., Karila, K., Koivumäki, N., Pelto-
1350 Arvo, M., Tuviala, J., Östersund, M., Pölönen, I., Lyytikäinen-Saarenmaa, P., 2023. Comparison of Deep
1351 Neural Networks in the Classification of Bark Beetle-Induced Spruce Damage Using UAS Images.
1352 *Remote Sensing* 15, 4928. <https://doi.org/10.3390/rs15204928>
- 1353 Walden, L., Fontaine, J.B., Ruthrof, K.X., Matusick, G., Harper, R.J., 2023. Drought then wildfire reveals a
1354 compound disturbance in a resprouting forest. *Ecological Applications* 33, e2775.
1355 <https://doi.org/10.1002/eap.2775>

- 1356 Wang, G., Mo, C., Li, Y., Huang, J., Song, W., 2025a. Dual-stream feature integration network for unmanned
1357 aerial vehicles remote sensing detection of dense standing dead trees. *Computers and Electronics in*
1358 *Agriculture* 236, 110468. <https://doi.org/10.1016/j.compag.2025.110468>
- 1359 Wang, Q., Zhao, Y., Che, Y., Shen, H., Qiu, Y., Wang, Y., 2026. A semi-supervised framework for UAV-based
1360 individual tree crown segmentation in structurally heterogeneous planted forests. *International*
1361 *Journal of Applied Earth Observation and Geoinformation* 146, 105078.
1362 <https://doi.org/10.1016/j.jag.2025.105078>
- 1363 Wang, R., Ma, L., He, G., Johnson, B.A., Yan, Z., Chang, M., Liang, Y., 2024. Transformers for Remote Sensing: A
1364 Systematic Review and Analysis. *Sensors* 24. <https://doi.org/10.3390/s24113495>
- 1365 Wang, X., Zhao, Q., Jiang, P., Zheng, Y., Yuan, L., Yuan, P., 2022. LDS-YOLO: A lightweight small object detection
1366 method for dead trees from shelter forest. *Computers and Electronics in Agriculture* 198, 107035.
1367 <https://doi.org/10.1016/j.compag.2022.107035>
- 1368 Wang, Z., Li, C., Wang, R., Ma, L., Hurtt, G., Jia, X., Mai, G., Li, Z., Xie, Y., 2025b. TreeFinder: A US-Scale
1369 Benchmark Dataset for Individual Tree Mortality Monitoring Using High-Resolution Aerial Imagery, in:
1370 *The Thirty-Ninth Annual Conference on Neural Information Processing Systems Datasets and*
1371 *Benchmarks Track*.
- 1372 Weinstein, B.G., Marconi, S., Bohlman, S., Zare, A., White, E., 2019. Individual Tree-Crown Detection in RGB
1373 Imagery Using Semi-Supervised Deep Learning Neural Networks. *Remote Sensing* 11, 1309.
1374 <https://doi.org/10.3390/rs11111309>
- 1375 Weinstein, B.G., Marconi, S., Bohlman, S.A., Zare, A., Singh, A., Graves, S.J., White, E.P., 2021. A remote
1376 sensing derived data set of 100 million individual tree crowns for the National Ecological Observatory
1377 Network. *eLife* 10, e62922. <https://doi.org/10.7554/eLife.62922>
- 1378 White, J., Wulder, M., Vastaranta, M., Coops, N., Pitt, D., Woods, M., 2013. The Utility of Image-Based Point
1379 Clouds for Forest Inventory: A Comparison with Airborne Laser Scanning. *Forests* 4, 518–536.
1380 <https://doi.org/10.3390/f4030518>
- 1381 Wijas, B.J., Allison, S.D., Austin, A.T., Cornwell, W.K., Cornelissen, J.H.C., Eggleton, P., Fraver, S., Ooi, M.K.J.,
1382 Powell, J.R., Woodall, C.W., Zanne, A.E., 2024. The Role of Deadwood in the Carbon Cycle:
1383 Implications for Models, Forest Management, and Future Climates. *Annual Review of Ecology,*
1384 *Evolution, and Systematics* 55, 133–155. <https://doi.org/10.1146/annurev-ecolsys-110421-102327>
- 1385 Wong, T.-C., Sani-Mohammed, A., Wang, J., Wang, P., Yao, W., Heurich, M., 2024. Classification of single tree
1386 decay stages from combined airborne LiDAR data and CIR imagery. *Geo-spatial Information Science*
1387 27, 2076–2091. <https://doi.org/10.1080/10095020.2024.2311861>
- 1388 Wulder, M.A., White, J.C., Ortlepp, S.M., Mora, B., Coggins, S., Coops, N.C., Heath, J., 2012. Digital high spatial
1389 resolution aerial imagery to support forest health monitoring: the mountain pine beetle context. *JARS*
1390 6, 062527. <https://doi.org/10.1117/1.JRS.6.062527>
- 1391 Xu, Z., Jiang, D., 2025. AI-Powered Plant Science: Transforming Forestry Monitoring, Disease Prediction, and
1392 Climate Adaptation. *Plants* 14, 1626. <https://doi.org/10.3390/plants14111626>
- 1393 Yang, C., Lu, J., Fu, H., Guo, W., Shao, Z., Li, Y., Zhang, M., Li, X., Ma, Y., 2025. Detection of Pine Wilt Disease-
1394 Infected Dead Trees in Complex Mountainous Areas Using Enhanced YOLOv5 and UAV Remote
1395 Sensing. *Remote Sensing* 17, 2953. <https://doi.org/10.3390/rs17172953>
- 1396 Yang, J., Tian, H., Pan, S., Chen, G., Zhang, B., Dangal, S., 2018. Amazon drought and forest response: Largely
1397 reduced forest photosynthesis but slightly increased canopy greenness during the extreme drought of
1398 2015/2016. *Global Change Biology* 24, 1919–1934. <https://doi.org/10.1111/gcb.14056>

1399 Yao, S., Hao, Z., Post, C.J., Mikhailova, E.A., Lin, L., 2024. Individual Tree Crown Detection and Classification of
1400 Live and Dead Trees Using a Mask Region-Based Convolutional Neural Network (Mask R-CNN). *Forests*
1401 15, 1900. <https://doi.org/10.3390/f15111900>

1402 Yun, T., Li, J., Ma, L., Zhou, J., Wang, R., Eichhorn, M.P., Zhang, H., 2024. Status, advancements and prospects
1403 of deep learning methods applied in forest studies. *International Journal of Applied Earth Observation*
1404 and *Geoinformation* 131, 103938. <https://doi.org/10.1016/j.jag.2024.103938>

1405 Zhang, L., Gao, X., Zhou, S., Zhang, Z., Zhao, T., Cai, Y., Zhao, X., 2025a. Identification of standing dead trees in
1406 Robinia pseudoacacia plantations across China's Loess Plateau using multiple deep learning models.
1407 *International Journal of Applied Earth Observation and Geoinformation* 136, 104388.
1408 <https://doi.org/10.1016/j.jag.2025.104388>

1409 Zhang, Y., Peng, Z., Song, Z., Schilling, J.S., 2025b. Repeated measures of decaying wood reveal the success
1410 and influence of fungal wood endophytes. *mSystems* 10, e00382-25.
1411 <https://doi.org/10.1128/msystems.00382-25>

1412 Zhao, H., Morgenroth, J., Pearse, G., Schindler, J., 2023. A Systematic Review of Individual Tree Crown
1413 Detection and Delineation with Convolutional Neural Networks (CNN). *Curr Forestry Rep* 9, 149–170.
1414 <https://doi.org/10.1007/s40725-023-00184-3>

1415 Zheng, Y., Hu, Z., Jian, J., Chen, J., Osborne, B.B., Zhou, G., Xu, Q., Zheng, Z., Ma, L., He, X., Bell, S.M., Frew, A.,
1416 2025. Tree functional group mediates the effects of nutrient addition on soil nutrients and fungal
1417 communities beneath decomposing wood. *Plant Soil* 510, 797–813. [https://doi.org/10.1007/s11104-](https://doi.org/10.1007/s11104-024-06959-2)
1418 [024-06959-2](https://doi.org/10.1007/s11104-024-06959-2)

1419 Zhou, H., Wu, S., Xu, Z., Sun, H., 2024. Automatic detection of standing dead trees based on improved YOLOv7
1420 from airborne remote sensing imagery. *Front. Plant Sci.* 15, 1278161.
1421 <https://doi.org/10.3389/fpls.2024.1278161>

1422 Zhou, L., Dai, L., Gu, H., Zhong, L., 2007. Review on the decomposition and influence factors of coarse woody
1423 debris in forest ecosystem. *J. of For. Res.* 18, 48–54. <https://doi.org/10.1007/s11676-007-0009-9>

1424 Zielewska-Büttner, K., Heurich, M., Müller, J., Braunisch, V., 2018. Remotely Sensed Single Tree Data Enable
1425 the Determination of Habitat Thresholds for the Three-Toed Woodpecker (*Picoides tridactylus*).
1426 *Remote Sensing* 10. <https://doi.org/10.3390/rs10121972>

1427

1428

1429

1430

1431

1432

1433

1434

1435

1436

1437

1438 **Appendix A.**

1439 **Table A1.** Literature identification, screening, and inclusion process for the review

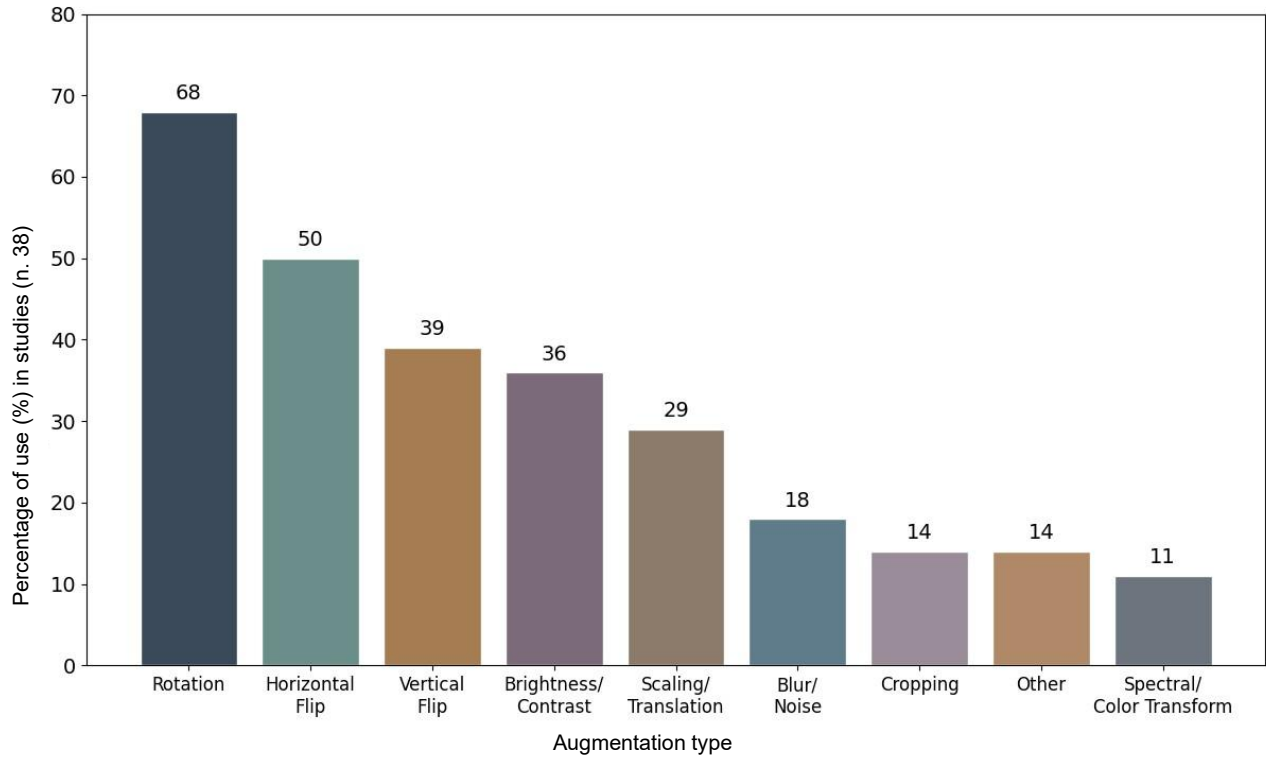
1440

Review stage	Screening step	Records, n	Description / criteria
Identification	Records retrieved from Scopus	59	Search applied to titles, abstracts, and keywords using structured Boolean terms related to standing dead trees, deadwood, tree mortality, deep learning, and remote sensing.
Identification	Records retrieved from Google Scholar	80	Simplified keyword combinations were used because Google Scholar does not support the same structured Boolean syntax as Scopus.
Identification	Total records retrieved before deduplication	139	Total number of records retrieved from Scopus and Google Scholar before duplicate removal.
Deduplication / preliminary screening	Duplicate and clearly irrelevant records removed	74	Duplicate records and records clearly outside the scope of the review were removed before detailed screening.
Screening	Records screened by title and abstract	65	Records screened for relevance to standing dead trees, dead-tree crowns, snags, tree mortality, deep learning, and remotely sensed data.
Screening	Records excluded after title and abstract screening	7	Records excluded because they were unrelated to standing dead trees, did not use deep learning, did not use remote sensing, or focused only on general forest disturbance.
Eligibility	Full-text records assessed for eligibility	58	Full texts were assessed against the inclusion and exclusion criteria.
Eligibility	Full-text records excluded	20	Records excluded because they lacked a deep learning method, did not use remotely sensed data, focused only on fallen deadwood, addressed general disturbance without a standing-dead-tree target, or lacked sufficient methodological detail.

Included	Studies included in final review	38	Studies included in the final synthesis of deep-learning-based standing dead-tree detection and mapping.
----------	----------------------------------	----	--

1441

1442



1443

1444 **Fig. A1.** Percentage of reviewed studies reporting each augmentation type; studies may report multiple
1445 augmentations.

1446

1447 **Table A2.** Validation approaches used in the reviewed standing dead-tree mapping studies.

Validation type	Studies
Image interpretation-based	Mosig et al., 2026; Ferrari et al., 2026; Möhring et al., 2025; Ahishali et al., 2025; Wang et al., 2025; Rahman et al., 2025; Yang et al., 2025; L. Zhang et al., 2025; Gonzalez and Wallner, 2025; Leidemer et al., 2025; Junttila et al., 2024; Wong et al., 2024; Cheng et al., 2024; Zhou et al., 2024; Yao et al., 2024; Lucas et al., 2024; Khatri-Chhetri et al., 2024; Schwarz et al., 2024; Jin et al., 2023; Jiang et al., 2023; Dixon et al., 2023; Schiefer et al., 2023; Turkulainen et al., 2023; Sani-Mohammed et al., 2022; Han et al., 2022; Wang et

Validation type	Studies
	al., 2022; Hell et al., 2022; Briechle et al., 2021; Tao et al., 2020; Chiang et al., 2020; Briechle et al., 2020; Deng et al., 2020; Sylvain et al., 2019; Jiang et al., 2019
Mixed (field + image)	Mäyrä et al., 2025; Matejčíková et al., 2024; Jääskeläinen, 2024; Fricker et al., 2019

1448

1449